Liu *et al. Biology Direct* (2025) 20:38
https://doi.org/10.1186/s13062-025-00631-0

Biology Direct

RESEARCH Open Access

Identification of druggable targets in acute kidney injury by proteome- and transcriptome-wide Mendelian randomization and bioinformatics analysis

Jiachen Liu[1,2†], Dianjie Zeng[1,3,4†], Yinhuai Wang[1], Fei Deng[1,3], Shuiqing Wu[1*] and Zebin Deng[1,3*]

Abstract

Background Acute kidney injury (AKI) remains a critical condition with limited therapeutic options, predominantly managed by renal replacement therapy. The challenge of developing targeted treatments persists.

Methods We integrated genetic data related to druggable proteins and gene expression with AKI genome-wide association study (GWAS) findings. Based on multi-omics Mendelian randomization (MR), we identified the potential causal influence of 5,883 unique proteins and genes on AKI. We also performed using reverse MR and external cohort-based analysis to verify the robustness of this causal relationship. Expression patterns of these targets were examined using bulk transcriptome and single-cell transcriptome data. In addition, drug repurposing analyses were conducted to explore the potential of existing medications. We also constructed a molecular interaction network to explore the interplay between identified targets and known drugs.

Results Genetically predicted levels of seven proteins and twelve genes were associated with an increased risk of AKI. Of these, six targets (*NCF1*, *TNFRSF1B*, *APEH*, *ACADSB*, *ADD1*, and *FAM3B*) were prioritized based on robust evidence and validated in independent cohorts. Reverse MR showed a one-way causal relationship of targets. These targets are predominantly expressed in proximal tubular cells, endothelial cells, collecting duct-principal cells, and immune cells within both AKI-affected and normal tissues. Several promising drug repurposing opportunities were identified, such as telmisartan-*NCF1*, calcitriol-*ACADSB*, and ethinyl estradiol-*ACADSB*. The molecular interaction mapping and pathway integration analysis provided further insights, suggesting potential strategies for combinatorial therapies.

Conclusions This extensive investigation identified several promising therapeutic targets for AKI and highlighted opportunities for drug repurposing. These findings offer valuable insights that could shape future research and the development of targeted treatments.

†Jiachen Liu and Dianjie Zeng co first authors.

*Correspondence:
Shuiqing Wu
wushuiqing@csu.edu.cn
Zebin Deng
zebindeng@csu.edu.cn

Full list of author information is available at the end of the article

© The Author(s) 2025. **Open Access** This article is licensed under a Creative Commons Attribution-NonCommercial-NoDerivatives 4.0 International License, which permits any non-commercial use, sharing, distribution and reproduction in any medium or format, as long as you give appropriate credit to the original author(s) and the source, provide a link to the Creative Commons licence, and indicate if you modified the licensed material. You do not have permission under this licence to share adapted material derived from this article or parts of it. The images or other third party material in this article are included in the article's Creative Commons licence, unless indicated otherwise in a credit line to the material. If material is not included in the article's Creative Commons licence and your intended use is not permitted by statutory regulation or exceeds the permitted use, you will need to obtain permission directly from the copyright holder. To view a copy of this licence, visit http://creativecommons.org/licenses/by-nc-nd/4.0/.

Keywords Acute kidney injury, Proteomics, Transcriptomics, Mendelian randomization, Bioinformatics, Drug repositioning

Background

Acute kidney injury (AKI) is a clinical syndrome characterized by a rapid decline in renal excretory function [1], affecting over one-fifth of hospitalized adults and one-third of hospitalized children globally [2]. Patients with AKI face heightened risks of both short-term and long-term mortality [3], as well as increased susceptibility to cardiovascular complications [4], chronic kidney disease [5], and end-stage renal disease [6]. This significantly impacts survivors' quality of life, often leading to work disabilities and considerable post-AKI medical expenses. Currently, a general management principle for AKI patients is fluid balance management, including necessary fluid resuscitation [7], which is essential for preventing further kidney damage and promoting recovery [8]. For severe AKI, particularly in critically ill patients, renal replacement therapy remains the predominant treatment [9]. However, this approach is primarily reserved for life-threatening conditions and cannot reverse the pathological progression of AKI [10].

The development of pharmacological treatments for AKI represents an emerging and promising area of research. However, the pathophysiology of AKI encompasses multiple overlapping yet distinct pathways, such as oxidative stress [11], inflammatory response [12], cell death [13], and immune response [14]. The complexity of its pathogenesis, coupled with patient heterogeneity, has significantly impeded progress in drug development. To date, most drugs for AKI remain in clinical trials, demonstrating uncertain efficacy and potential side effects [15], suggesting that widespread clinical use remains a distant goal. Given the escalating global incidence of AKI [16], there is an urgent need for more targeted and effective therapies to mitigate its adverse outcomes and socioeconomic burden.

Precision medicine, grounded in molecularly targeted therapies, offers valuable insights into the treatment of AKI [17, 18]. Given the potential contribution of genetic factors to AKI susceptibility and severity, personalized targeted therapies tailored to patients with diverse genetic backgrounds may represent a novel approach to managing AKI in the future [19]. Large-scale human genetic studies, enabled by the continuous advancement of gene sequencing technology, present opportunities for the development of targeted therapies for AKI. Previous genome-wide association studies (GWASs) have successfully identified single nucleotide polymorphisms (SNPs) associated with AKI risk by analyzing the genetic backgrounds of tens of thousands of individuals affected by AKI [20, 21]. However, these loci are upstream of biological mechanisms and are distant from being viable therapeutic targets. Genes encoding druggable human proteins can offer valuable clues for drug target discovery [22]. Nevertheless, identifying prospective targets from observational studies can be challenging due to the risk of confounding or reverse causation bias.

Mendelian randomization (MR), an innovative genetic statistical method for causal inference, can effectively avoid the confounding bias inherent in observational studies [23]. By integrating GWAS data of AKI with protein/expression quantitative trait loci (pQTL/eQTL) data, MR can assess whether genetically predicted variations in protein or gene expression levels have a causal role in AKI risk. Recent studies have effectively utilized druggable QTL data and disease GWAS data to elucidate the underlying mechanisms of complex diseases and to provide insights into novel targets [24–26].

Consequently, the primary objective of this study was to identify causal biomarkers and potential therapeutic targets for AKI. By integrating pQTL and eQTL data from druggable genes, we estimated their potential causal effects on AKI using MR and colocalization analysis. Transcript-level analysis was performed to further elucidate our findings. Subsequently, drug-repurposing assessments were conducted through database queries and molecular docking to identify promising drugs. Finally, a protein-protein interaction (PPI) network and enrichment analyses were utilized to further explore the association between candidate targets and experimental AKI drug targets, providing novel insights into multi-target combination therapies.

Methods

Study design

The study design is depicted in Fig. 1. The data collected in this study came from FinnGen Consortium and other public databases; the data were desensitized before uploading and did not involve personal privacy or identifiable information. This study did not involve information and data and informed consent authorization of the institution, so no ethical review was not necessary.

Data source

Data source for AKI

We leveraged a recently released large-scale GWAS focusing on AKI [27], which was derived from a dataset consisting of 7,695 individuals of European ancestry diagnosed with AKI and 482,266 controls of European ancestry. We used summary statistics from the FinnGen Consortium (R9) (https://www.finngen.fi/en) for exter

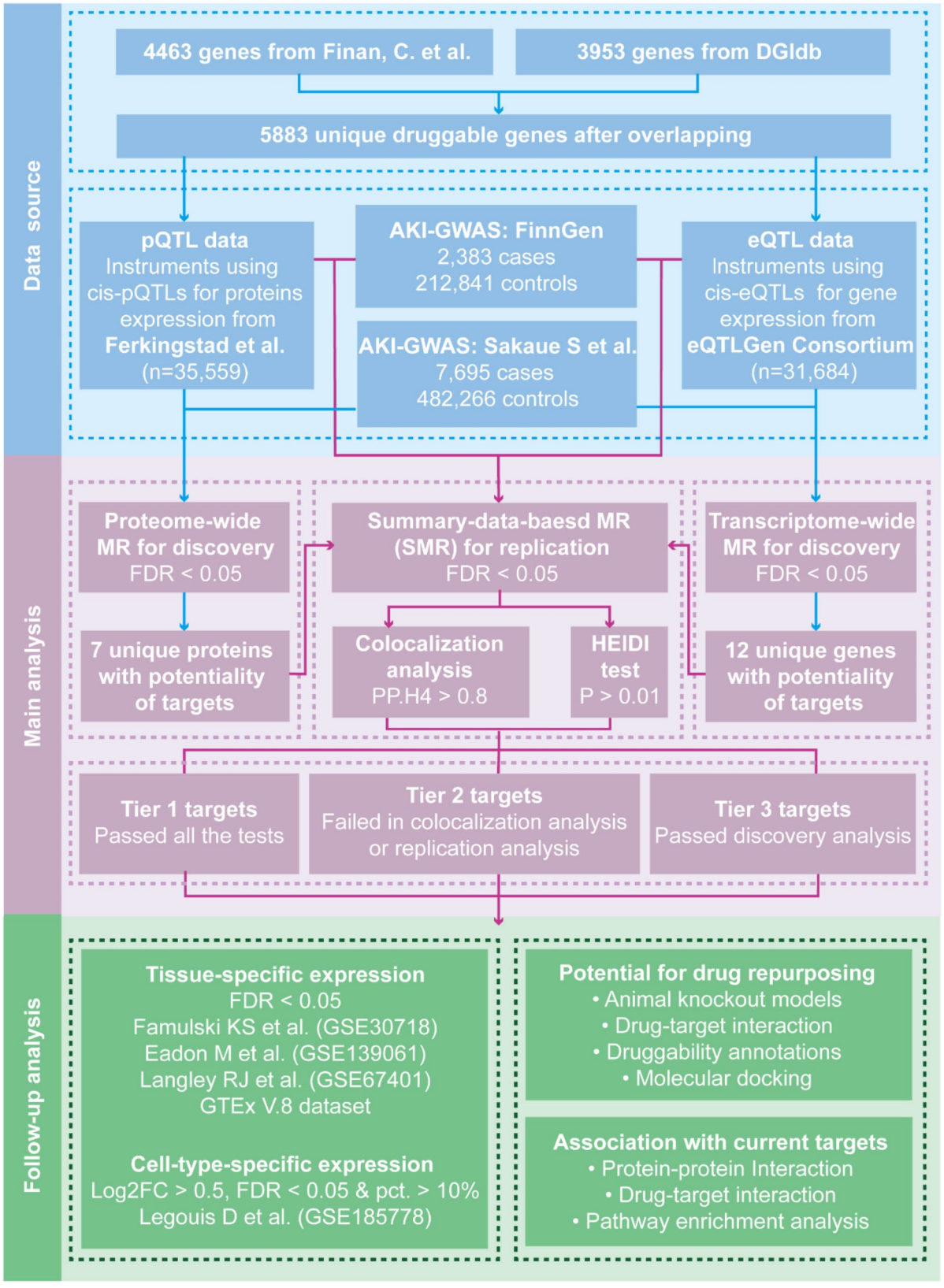

Fig. 1 Flowchart of the study design. AKI, acute kidney injury; MR, Mendelian randomization; PWMR, proteome-wide MR analysis; TWMR, transcriptome-wide MR analysis; GWAS, genome-wide association study; pQTL, protein quantitative trait loci; eQTL, expression quantitative trait loci; SMR, summary-data-based mendelian randomization; PP.H4, posterior probability of H4; HEIDI, heterogeneity in dependent instruments; FDR, false discovery rate

nal replication in an independent sample cohort which included 2,383 individuals with AKI, and 212,841 controls. Regarding transcript-level data, the publicly accessible bulk RNA-seq data were obtained from Famulski KS et al. (28 AKI samples and 19 controls) [28], Eadon M et al. (39 AKI samples and nine controls) [29], Langley RJ et al. (53 AKI samples and 58 controls) [30], and the Genotype Tissue Expression V.8 dataset (GTEx, https://gtexportal.org/). Human single-cell nuclear RNA-seq data for AKI were provided by Legouis D et al. (two AKI samples and three controls) [31]. Details are provided in Table S1.

Identification of druggable genes

We identified druggable genes using data from the Drug–Gene Interaction Database (DGIdb, version 4.2.0, https://www.dgidb.org/). We downloaded the "Categories Data" released in February 2022, which includes all genes classified as druggable in the DGIdb and mapped to Entrez genes. Additionally, we referenced a list of druggable genes provided in the review by Finan et al. [22]. The list of druggable genes is shown in Table S2.

Plasma protein/expression quantitative trait loci (pQTL/eQTL) data

Genetic instrumental variables for the proteome were reported by Ferkingstad et al. [32]. Their study represents the largest pQTL analysis to date, encompassing 4,907 proteins studied in 35,559 individuals of Icelandic descent. The analysis identified 18,084 associations between genetic variants and plasma protein levels. Subsequently, pQTLs were extracted from the deCODE study using aria2c (http://aria2.sourceforge.net/). Besides, to mitigate concerns of horizontal pleiotropy, instrumental variables were restricted to cis-pQTLs (SNPs located within a 1,000 kb window around the target gene) for each protein. To generate eQTL instruments, genetic variants located within 1,000 kb on either side of the coding sequence (in cis) that are robustly associated with gene expression were extracted using eQTLs summary statistics obtained from the eQTLGene Consortium [33]. Details of these studies are presented in Table S1.

Main analysis

Multi-omics MR analysis

The validity of MR rests on three key assumptions: (1) Instrumental variables must be associated with the exposure; (2) Instrumental variables must not be associated with potential confounders; and (3) Instrumental variables affect the outcome solely through their influence on the exposure [34]. To meet the assumptions presented earlier, we first mapped single-nucleotide polymorphisms (SNPs) to human genome Build 37 (GRCh37) for unifying genomic coordinates, and then rigorously derived instrumental variables from druggable pQTL and eQTL data as follows: (1) SNPs associated with each exposure were chosen based on genome-wide significance ($P < 5 \times 10^{-8}$). (2) Cis-acting SNPs (cis-QTLs) located within 1,000 kb of transcription start sites for proteins and genes were chosen. Compared with the trans instruments, the cis instruments were less likely to violate the horizontal pleiotropy assumption [35]. (3) SNPs within the human major histocompatibility complex (MHC) region (chr6: from 26 Mb to 34 Mb) were removed, as the linkage disequilibrium (LD) patterns of SNPs in the MHC region are complex [35]. (4) Linkage disequilibrium analysis was conducted within a 10,000 kb window to remove SNPs with an $r^2 > 0.001$. (5) Strength of each SNP as an instrument was assessed using the F-statistic, calculated as mean β^2/σ^2, where β represents the effect size of SNP on the exposure (i.e., the allelic difference in exposure) and σ is the standard error of β. A high F-statistic (> 10) indicates minimal risk of weak instrument bias, which is crucial in MR studies [36]. Thus, only SNPs with F-statistics exceeding 10 were retained for further analysis. (6) SNPs with ambiguous palindromic structures were removed to avoid ambiguity.

We also looked up each instrumental variable and its proxies in the PhenoScanner GWAS database (http://phenoscanner.medschl.cam.ac.uk) to assess any associations with potential confounders (education, smoking, drinking, blood pressure, and socioeconomic status). SNPs associated with potential confounders were removed ($P < 1 \times 10^{-5}$). The remaining SNPs were used to perform MR analysis. The Wald ratio was used if only one genetic instrumental variable was available for a given protein or gene, and the inverse-variance weighted method was applied when two or more instrumental variables were available. Significance of MR analysis was determined using false discovery rate (FDR)-corrected (FDR = 0.05).

Sensitivity analysis and reverse MR

Sensitivity analysis was used to verify the robustness of the results. For proteins or genes with more than two instrumental variables, Cochran's Q and I^2 statistic were calculated to test for heterogeneity. A significant p-value ($P < 0.05$) indicates the presence of heterogeneity [37]. If heterogeneity was present, the random-effects model of the inverse-variance weighted method was used, otherwise inverse-variance weighted method with fixed effects was applied. The presence of horizontal pleiotropy was tested using MR-Egger regression when three or more instrumental variables were included [38], and cis-QTLs with a significant MR-Egger regression intercept ($P < 0.05$) would be removed. Moreover, to evaluate the impact of LD pruning choices, we performed MR analyses using alternative pruning windows (500 kb). Steiger filtering and reverse MR were conducted to check whether the MR analysis estimates assessed

the true causal direction [39]. SNPs with a Steiger test p-value < 0.05 and a reversed causal direction (i.e., R^2_outcome > R^2_exposure) were removed. The significance threshold for reverse MR analysis was set at FDR = 0.05 to detect potential reverse causality. Both the "Two Sample MR" and "MR-PRESSO" packages in R software (version 4.3.1) were used to estimate the MR and sensitivity findings [39, 40].

Colocalization analysis

Colocalisation analysis was conducted to determine if the associations between specific protein abundance or gene expressions and AKI were attributable to the same causal genetic variant. Colocalisation uses computed approximation Bayes factors and summary association data; the five mutually exclusive hypotheses were tested, which were as follows: (1) no causal SNP was found for either AKI GWAS or QTL (H0); (2) only AKI GWAS had a causal SNP (H1); (3) only QTL had a causal SNP (H2); (4) AKI GWAS and QTL had a causal SNP; however, the two causal SNPs differed (H3); (5) AKI GWAS and QTL had a causal SNP and shared the same SNP (H4). For proteomic or transcriptomics traits where an instrumental variable was located within a cis region (+/- 1 Mb) of the gene target, colocalization analysis was conducted using coloc [41]. Based on empirical evidence from similar studies, prior probabilities (p_1, $p_2 = 1 \times 10^{-4}$ and $p_{12} = 1 \times 10^{-5}$) were adopted [24, 25], and a posterior probability ≥ 0.80 was considered indicative of strong support for a specific model. Additionally, we conducted a sensitivity analysis by varying prior probabilities (p1, $p2 = 1 \times 10^{-3}$ and 1×10^{-5}) to evaluate the robustness of our colocalization findings.

Replication analysis based on FinnGen consortium research

We replicated the primary MR analysis of druggable proteins and genes on AKI based on different GWAS data sources using Summary-based Mendelian randomization (SMR) analysis. As an extension of the MR concept, Summary-based Mendelian randomization was developed to estimate the pleiotropic association between genetically determined traits (e.g., gene expression, DNA methylation, or protein abundance as exposure) and complex traits of interest (e.g., disease phenotype as outcome) [42]. Here, we performed SMR using the Linux version 1.0.3 of SMR software in the command line using default options (https://yanglab.westlake.edu.cn/software/smr/). HEIDI test was performed, which incorporates significant SNPs other than the top SNP in the cis-QTL region to test whether genetic associations were due to LD. Results with HEIDI *P*-value < 0.01 were considered due to linkage rather than functional association.

Follow-up analysis

Bulk transcriptomic validation and tissue-specific expression

To observe the actual expression of identified genes, we analyzed publicly available bulk RNA-seq data from Famulski KS et al. [28], which included 28 AKI renal tissue samples and 19 normal renal tissue samples. After extracting the gene expression matrix and grouping information from the dataset, we normalized, annotated, and cleaned the data using the "limma" package [43]. To assess the overall expression differences of target genes between AKI and normal tissues, we extracted their expression levels from the processed expression matrix and compared the two groups using an unpaired Student's t-test. Multiple comparisons were adjusted using the Benjamini-Hochberg method. To validate our findings, we performed replication analyses using an alternative approach (limma) and additional datasets (Eadon M et al. and Langley RJ et al.) [29, 30], respectively. In addition, we obtained bulk RNA-seq data representing 53 different tissues from the Genotype-Tissue Expression (GTEx, https://gtexportal.org/) project, and visualised the expression levels of each gene in different tissues.

Single-cell nuclear transcriptomic validation and cell-type-specific expression

We examined the cell-type-specific expression of the candidate genes using human AKI single-cell nuclear RNA-seq data profiled by Legouis D et al. [31]. The raw snRNA-seq data were first subjected to preprocessing and conversion using the "Seurat" package [44]. After filtering low-quality data, including nuclei with fewer than 150 nFeature_RNA detected or more than 4 times the absolute median of nFeature_RNA, we normalized the data using the "NormalizeData" function. Next, we used the "FindVariableFeatures" function to identify highly variable genes (HVGs) and the "RunPCA" function to perform principal component analysis (PCA) based on HVGs. The "Harmony" package was used to eliminate batch effects in expression data between different samples [45]. Subsequently, the "FindNeighbors" and "FindClusters" functions were used to cluster the cells. To annotate the cell clusters with cell types, we referred to relevant literature and the CellMarker 2.0 (http://bio-bigdata.hrbmu.edu.cn/CellMarker) to obtain cell types and their markers for human kidney tissues. Using the "FindAllMarkers" function, we assessed whether these genes were enriched in specific cell types. Finally, we visualized the expression levels of these candidate genes, identified differentially expressed genes in 10 renal cell types in AKI and normal tissues using a pseudobulk aggregation approach. The genes with an average Log2 fold change (Log2FC) more than 1, a false discovery rate (FDR) less than 0.05 were identified as differentially expressed genes.

Mouse knock-out models for druggable genes

To investigate evidence that modification of the target produces a phenotype relevant to AKI, we queried the Mouse Genome Informatics (MGI, http://www.informatics.jax.org/) database for candidate targets from our MR analysis, focusing on all systemic abnormalities associated with the knock-out (KO) mouse models. For abnormalities related to the renal/urinary system, we documented specific phenotypes in detail.

Drug repurposing assessment and molecular docking

Utilizing the DrugBank and ChEMBL databases [46, 47], we searched all targeted drugs associated with the candidate targets and systematically evaluated their potential for repurposing. By querying the Comparative Toxicogenomics Database (CTD) for the effects of drug interventions on protein levels and gene expression levels [48], we identified 56 additional potential drug candidates. To further validate the potential for drug repurposing and optimize the design of potential drug candidates, we conducted molecular docking to analyze the binding affinity and interaction patterns between drugs and their targets. The 3D structures of the target proteins were sourced from the Protein Data Bank (https://www.rcsb.org/), while the 3D structures of the drug molecules were retrieved from the PubChem database (https://pubchem.ncbi.nlm.nih.gov/). Subsequently, we employed AutoDock4 for molecular docking and utilized PyMol2.5 for visualization [49, 50].

Regarding molecular docking, the grid box was centered on the binding site of each target protein, with dimensions as follows: *NCF1* (30.0 × 30.0 × 30.0 Å), *TNFRSF1B* (48.0 × 44.0 × 64.0 Å), *APEH* (40.0 × 56.0 × 44.0 Å), *ACADSB* (42.0 × 40.0 × 50.0 Å), *ADD1* (42.0 × 36.0 × 48.0 Å), and *FAM3B* (30.0 × 25.0 × 32.0 Å). The grid spacing was set to 0.375 Å. The Lamarckian Genetic Algorithm (LGA) was used for docking, with a population size of 150, 2.5×10^6 energy evaluations, and 27,000 generations. The number of runs was set to 50 to ensure thorough sampling of the conformational space. The scoring function used was the AutoDock4 force field, which includes van der Waals, electrostatic, and hydrogen bonding terms. Default weighting parameters were applied for all energy terms. To validate the reliability of our docking protocol, we calculated the root-mean-square deviation (RMSD) between the predicted binding poses of drug candidates and their experimentally determined structures using PyMOL 2.5. The RMSD values less than 2 Å confirm the accuracy of our docking method.

Protein interaction and enrichment analysis with experimental drug targets

The ClinicalTrials.gov (https://clinicaltrials.gov/) was queried to identify approved or clinical-stage drugs currently promising for AKI. A protein-protein interaction network was constructed using the STRING database (https://cn.string-db.org/) and Cytoscape software to explore the possible connections between candidate targets and current clinical trial drug targets for AKI [51]. In addition, Gene Ontology (GO) and Kyoto Encyclopedia of Genes and Genomes (KEGG) enrichment analyses were performed to investigate the functional characteristics and biological relevance of these targets.

Results

Multi-omics MR analysis identified 19 causal biomarkers for AKI

To elucidate the functional relationships between genome-wide cis-pQTLs/eQTLs and AKI, we employed two sample MR to assess the associations (Table S3, S4). Seven proteins (*TNFRSF1B*, *ACADSB*, *FAM3B*, *LTF*, *TCN2*, *SLITRK6*, and *PNLIPRP2*) and twelve genes (*NCF1*, *APEH*, *ADD1*, *BRD9*, *ESR2*, *CDKN2C*, *EGFL8*, *ADC*, *LCN8*, *LPAR5*, *HSD17B3*, and *CD244*) passed our significance threshold (FDR < 0.05) (Fig. 2). Specifically, a positive correlation between genetically predicted plasma protein levels and AKI risk was detected for seven of the plasma proteins or genes: *LCN8* (Beta: 0.11, SE: 0.03, $p = 8.94E-04$), *NCF1* (Beta: 0.17, SE: 0.05, $p = 2.37E-03$), *ESR2* (Beta: 0.24, SE: 0.08, $p = 3.03E-03$), *BRD9* (Beta: 0.31, SE: 0.11, $p = 3.55E-03$), *EGFL8* (Beta: 0.34, SE: 0.12, $p = 3.95E-03$), *FAM3B* (Beta: 0.17, SE: 0.04, $p = 4.82E-05$), and *SLITRK6* (Beta: 0.25, SE: 0.08, $p = 2.61E-03$). The other 12 druggable proteins or genes showed a negative correlation with AKI risk: *CD244* (Beta: -0.16, SE: 0.05, $p = 2.73E-03$), *LPAR5* (Beta: -0.17, SE: 0.06, $p = 5.18E-03$), *APEH* (Beta: -0.24, SE: 0.06, $p = 8.22E-05$), *ADD1* (Beta: -0.34, SE: 0.11, $p = 1.89E-03$), *ADC* (Beta: -0.42, SE: 0.13, $p = 1.35E-03$), *HSD17B3* (Beta: -0.44, SE: 0.13, $p = 7.19E-04$), *CDKN2C* (Beta: -0.47, SE: 0.15, $p = 2.08E-03$), *TCN2* (Beta: -0.07, SE: 0.02, $p = 4.82E-03$), *PNLIPRP2* (Beta: -0.07, SE: 0.02, $p = 7.04E-03$), *TNFRSF1B* (Beta: -0.21, SE: 0.08, $p = 5.72E-03$), *LTF* (Beta: -0.22, SE: 0.07, $p = 2.01E-03$), and *ACADSB* (Beta: -0.52, SE: 0.18, $p = 3.65E-03$) (Table 1). Sensitivity analysis of MR estimates under 500KB LD clumping windows are shown in Table S5, which further supports the robustness of our results.

Moreover, the Cochrane's Q test and MR-Egger intercept test did not yield any significant findings of heterogeneity or pleiotropy among these proteins or genes ($P > 0.05$). In terms of reverse causation, no significant effects of AKI on plasma protein abundance or gene expression levels were found (Table 1), which demonstrates the robustness of the identified targets.

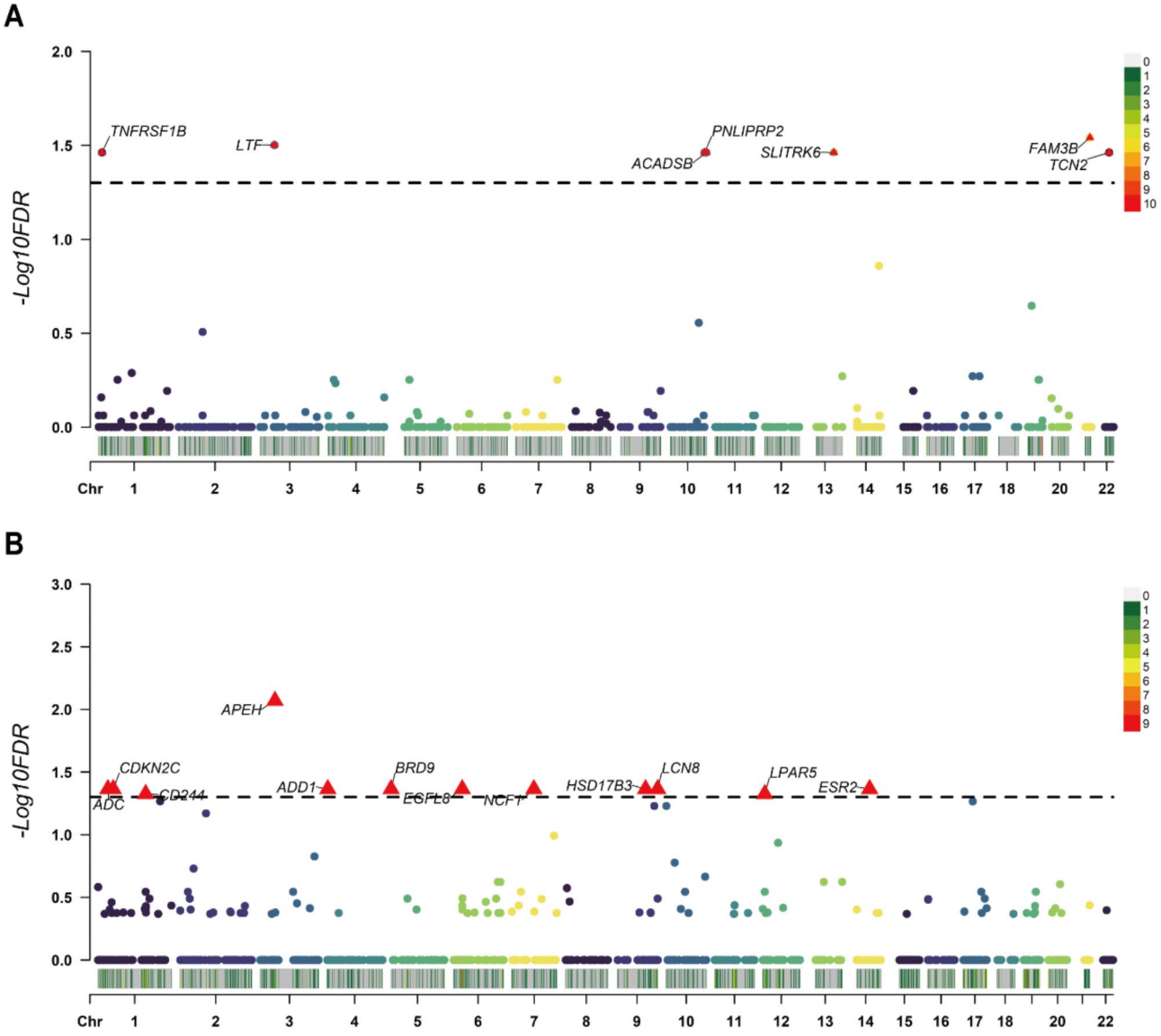

Fig. 2 Manhattan plots showing 19 causal biomarkers for AKI identified from PWMR and TWMR. (**A**) Manhattan plot showing the − log10(P.adj value) of association for each protein from the PWMR analysis plotted on the y-axis against genomic position on the x-axis. The dotted line corresponds to the significance threshold (Benjamini-Hochberg correction, *P.adj* < *0.05*). (**B**) Manhattan plot showing the − log10(P.adj value) of association for each gene from the TWMR analysis plotted on the y-axis against genomic position on the x-axis. The dotted line corresponds to the significance threshold (Benjamini-Hochberg correction, P.adj < 0.05)

Subsequently, we conducted several analyses to further minimize confounding and biases. For the proteins or genes that passed MR test, we performed genetic colocalization analysis to ensure the biomarkers were unlikely to be confounded by linkage disequilibrium (Figure S1). To further verify the observed findings, we performed SMR for these proteins or genes with GWAS summary statistics from external cohorts. The effect of all proteins or genes are presented in Table 2.

Among them, three proteins (*TNFRSF1B*, *ACADSB*, and *FAM3B*) and three genes (*NCF1*, *APEH*, and *ADD1*) passed the SMR test (Fig. 3A, B). We further used the HEIDI approach to test against the null hypothesis that the association detected by the SMR test is due to pleiotropy (*P*-HEIDI > 0.01). All the targets passed this evaluation. Besides, we found *TNFRSF1B*, *NCF1*, and *APEH* show strong evidence of colocalization (PP.H4 > 0.8), regardless of whether the priori probabilities (p1, p2) was 10^{-3},10^{-4}, or 10^{-5} (Fig. 3C-E, Table S6). None of the biomarkers that colocalized were within 500 KB of a known AKI GWAS loci. By integrating the findings from the main analyses, we categorized the identified proteins or genes into three tiers based on the strength of evidence. Tier 1 targets passed all tests, including MR, SMR, HEIDI

Table 1 Results of proteome-wide and transcriptome-wide MR, reverse MR and sensitivity analyses for acute kidney injury

Druggable	Target	Method	Nsnp	Beta	Se	*P*-value	$P_{heterogeneity}$	$P_{pleiotropy}$	$P_{reverse}$
Protein	TNFRSF1B	Inverse variance weighted	3	-0.21	0.08	5.72E-03	0.77	0.65	0.13
	ACADSB	Inverse variance weighted	2	-0.52	0.18	3.65E-03	0.40		0.35
	LTF	Inverse variance weighted	3	-0.22	0.07	2.01E-03	0.79	0.66	
	SLITRK6	Inverse variance weighted	4	0.25	0.08	2.61E-03	0.48	0.51	0.52
	TCN2	Inverse variance weighted	9	-0.07	0.02	4.82E-03	0.44	0.24	0.47
	FAM3B	Inverse variance weighted	4	0.17	0.04	4.82E-05	0.73	0.51	0.95
	PNLIPRP2	Inverse variance weighted	8	-0.07	0.02	7.04E-03	0.87	0.23	0.49
Gene	APEH	Inverse variance weighted	4	-0.24	0.06	8.22E-05	0.99	0.91	
	HSD17B3	Inverse variance weighted	2	-0.44	0.13	7.19E-04	0.34		
	LCN8	Inverse variance weighted	3	0.11	0.03	8.94E-04	0.63	0.64	
	ADC	Inverse variance weighted	3	-0.42	0.13	1.35E-03	0.43	0.42	
	ADD1	Inverse variance weighted	3	-0.34	0.11	1.89E-03	0.53	0.63	
	CDKN2C	Inverse variance weighted	2	-0.47	0.15	2.08E-03	0.92		
	NCF1	Inverse variance weighted	2	0.17	0.05	2.37E-03	0.60		
	CD244	Inverse variance weighted	6	-0.16	0.05	2.73E-03	0.93	0.77	
	ESR2	Inverse variance weighted	3	0.24	0.08	3.03E-03	0.66	0.53	
	BRD9	Inverse variance weighted	2	0.31	0.11	3.55E-03	0.62		
	EGFL8	Inverse variance weighted	2	0.34	0.12	3.95E-03	0.39		
	LPAR5	Inverse variance weighted	5	-0.17	0.06	5.18E-03	0.38	0.19	

Table 2 SMR results related to causal proteins and genes based on external cohort

Druggable	Target	Top snp	Beta	Se	*P*-value	P_{HEIDI}	PPH_4	Tier
Protein	TNFRSF1B	rs2301258	-0.31	0.14	1.09E-02	0.04	0.82	1
	ACADSB	rs7913063	-0.15	0.05	4.70E-03	0.16	0.09	2
	FAM3B	rs60265870	0.10	0.03	2.60E-03	0.92	0.04	2
	SLITRK6	rs9547179	-0.02	0.01	8.58E-02	0.40	0.22	3
	TCN2	rs4820885	0.00	0.00	6.70E-02	0.91	0.14	3
	PNLIPRP2	rs7910135	0.00	0.00	9.72E-01	0.84	0.09	3
Gene	NCF1	rs3846966	0.05	0.02	1.61E-02	0.37	0.86	1
	APEH	rs1131095	-0.03	0.01	2.01E-02	0.32	0.93	1
	ADD1	rs17833172	-0.01	0.00	3.10E-03	0.27	0.01	2
	LCN8	rs2282259	0.00	0.03	9.19E-01	0.87	0.04	3
	BRD9	rs28567708	0.06	0.12	5.95E-01	1.00	0.08	3
	CD244	rs1412849	-0.06	0.03	2.95E-02	0.16	0.07	3
	LPAR5	rs73264831	0.02	0.04	6.25E-01	0.70	0.15	3

test, and colocalization analysis. Tier 2 targets passed MR, SMR, and HEIDI test but not colocalization analysis. Tier 3 targets only passed MR. Based on this classification, *TNFRSF1B*, *NCF1*, and *APEH* were assigned to tier 1, while *ACADSB*, *FAM3B*, and *ADD1* were assigned to tier 2. The remaining 13 proteins or genes were classified as tier 3 targets.

Bulk transcriptomic validation and tissue-specific expression

Three significantly differentially expressed potential targets were identified in comparisons between AKI renal tissues and normal renal tissues: *ACADSB* (*P.adj* = 0.042), *LTF* (*P.adj* = 5.7E-04), and *APEH* (*P.adj* = 0.018). Additionally, *TNFRSF1B* (*P.adj* = 0.063) and *NCF1* (*P.adj* = 0.084) approached significance (Fig. 4A). Except for *ACADSB*, all these targets were significantly overexpressed in AKI renal tissues, indicating their potential involvement in the pathophysiological processes of AKI. Replication analyses using additional approach and datasets are provided in Figure S2, S3.

Subsequently, we utilized RNA-seq data from the GTEx to examine the expression of the aforementioned genes across various tissues. Most genes were considerably expressed in multiple tissues, including the kidney, and the expression levels in the blood exhibited clear differences. *ACADSB* expression was substantially lower in the blood compared to other tissues, whereas *TNFRSF1B* and *NCF1* demonstrated the opposite trend (Fig. 4B). The expression levels of other targets are shown in Figure S4.

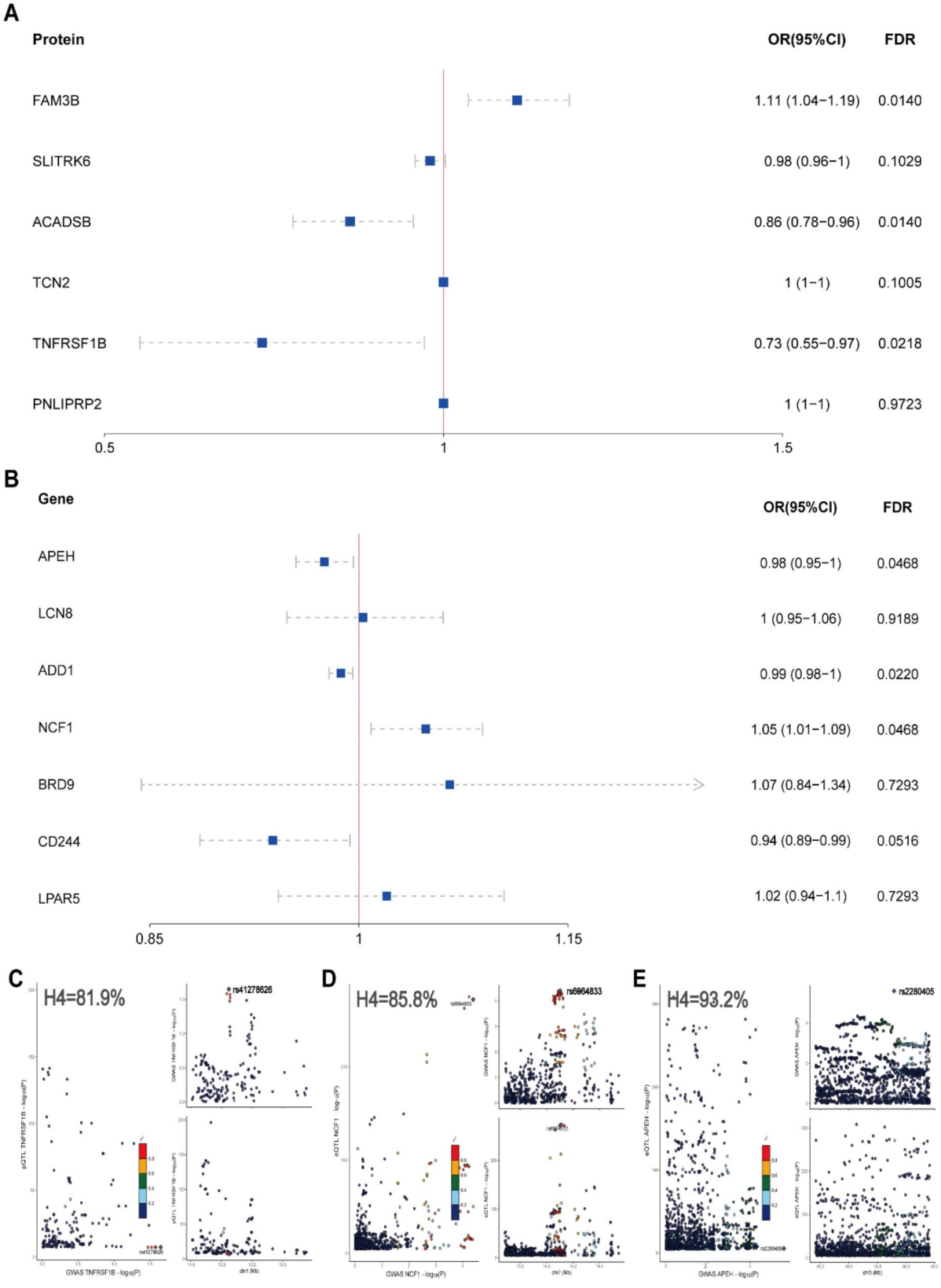

Fig. 3 SMR analysis and colocalisation evidence on the associations between PWMR-identified or TWMR-identified targets and the risk of AKI. (**A**) Forest plot shows the OR and P.adj value from proteome-wide SMR in the replication stage. (**B**) Forest plot shows the OR and P.adj value from transcriptome-wide SMR in the replication stage. (**C**) The colocalization result of TNFRSF1B. (**D**) The colocalization result of NCF1. (**E**) The colocalization result of APEH

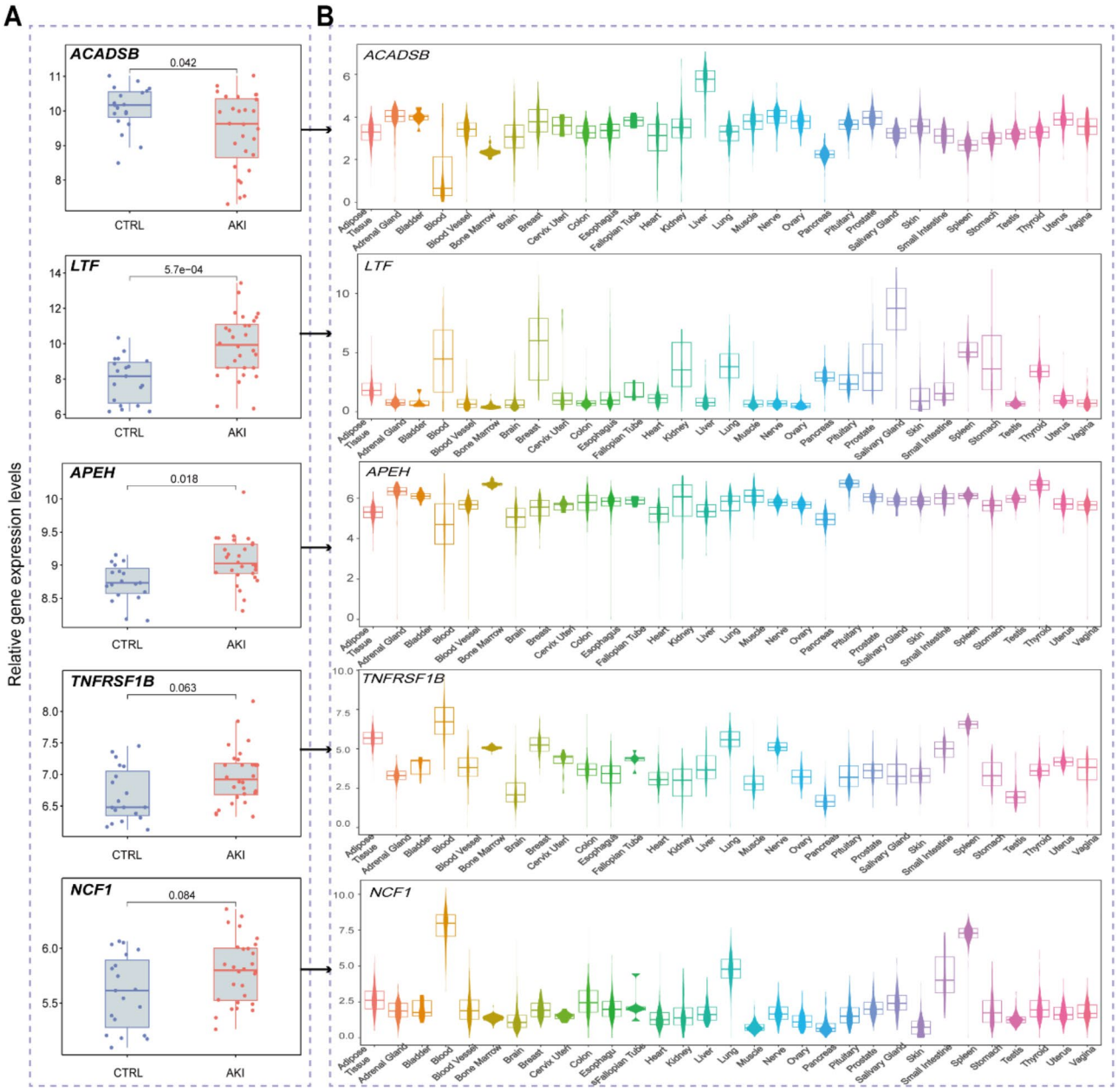

Fig. 4 Tissue-specific expression of identified targets. (**A**) Comparison of differences in relative expression of identified targets in AKI renal tissues and normal renal tissues in the GSE30718 dataset (Student's unpaired t-test, *P.adj* < *0.05*). (**B**) Expression levels of identified targets in different tissues from the GETx

Single-cell nuclear transcriptomic validation and cell-type-specific expression

We obtained 20,538 high-quality nuclei and classified them into ten distinct cell types: endothelial cells (Endo), podocytes (Podo), proximal tubular cells (PT), loop of Henle cells (LOH), distal convoluted tubular cells (DCT), collecting duct-principal cells (CD-PC), collecting duct-intercalated cells (CD-IC), renal progenitor cells (RPC), stromal cells, and immune cells (Fig. 5A, B). Among the druggable genes identified, expression data were available for 16 genes, while *ADC*, *SLITRK6*, and *PNLIPRP2* were not detected. Figure 5C displays the gene expression levels across each cell type in both AKI and normal tissues. In Fig. 6A and B, larger bubbles and darker colors represent higher expression levels of the corresponding targets on the same scale. To rigorously assess differential expression, we employed a pseudobulk aggregation approach, where cells within each sample were aggregated to create 'pseudobulk' profiles, followed by differential expression analysis using DESeq2. This analysis revealed that LTF was significantly up-regulated in specific cell types in AKI tissues compared to normal tissues

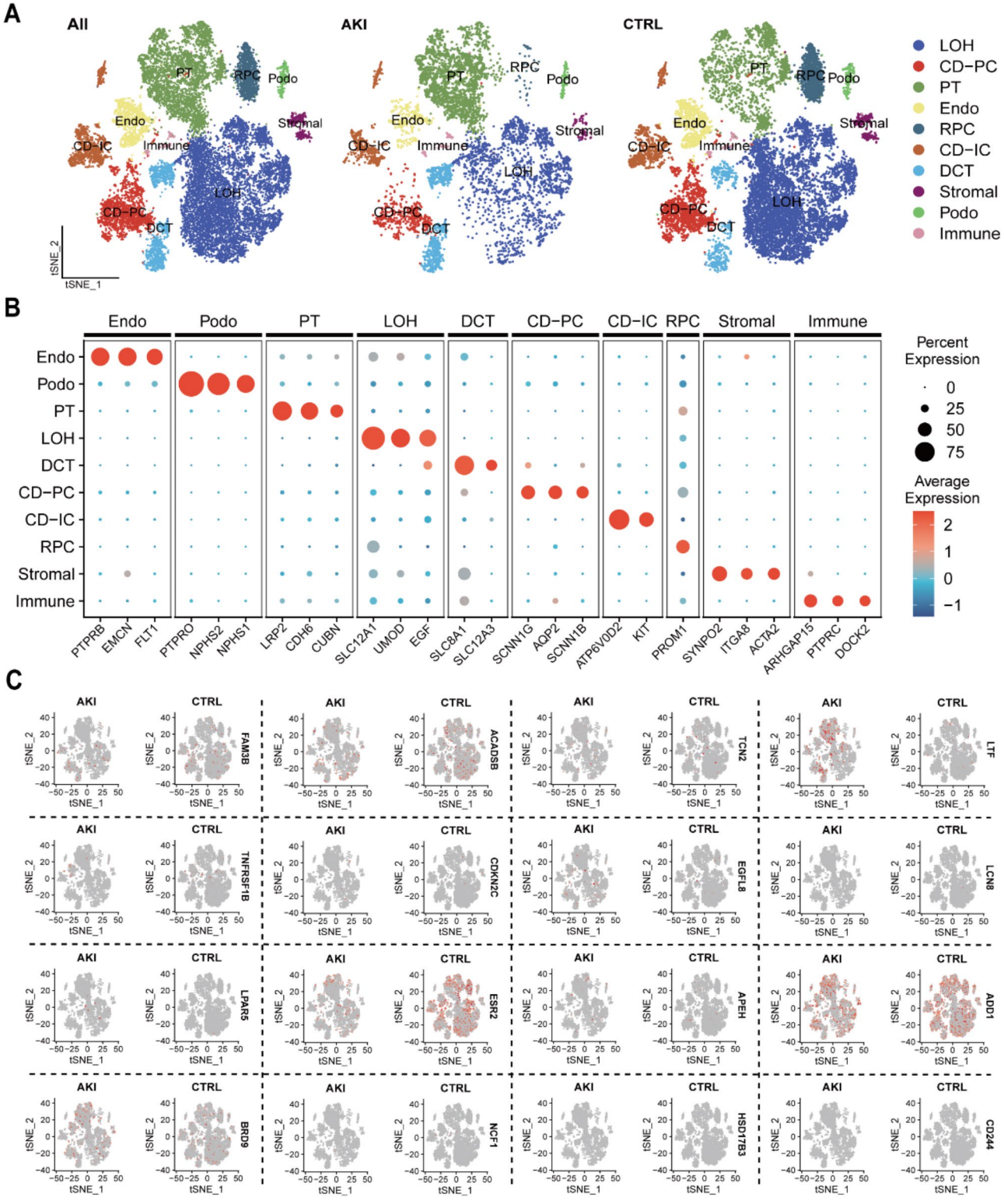

Fig. 5 Cell types contained in AKI renal tissue. (**A**) TSNE plot depicting ten distinct cell types identified in AKI and normal renal tissues. (**B**) Bubble chart showing average expression of known markers in indicated cell clusters. The dot size represents percent of cells expressing the genes in each cluster. (**C**) TSNE plots illustrating the expression levels of 16 identified targets

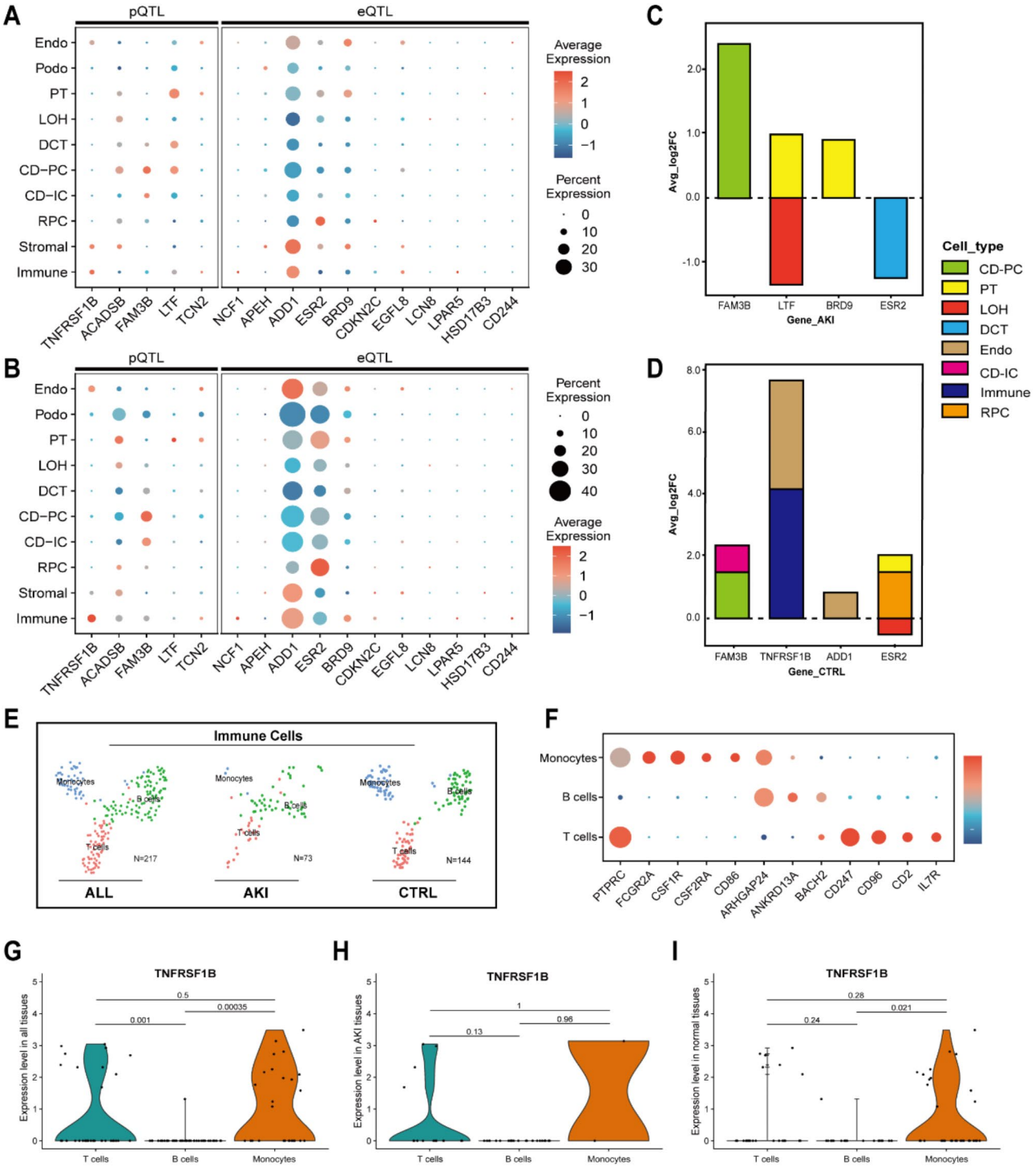

Fig. 6 Celltype-specific expression of identified targets in renal tissue. (**A**, **B**) Bubble chart illustrating the average expression levels of 16 identified targets in AKI tissues (**A**) and normal tissues (**B**). The dot size indicates the percentage of cells expressing the genes in each cluster. (**C**, **D**) Under the criteria of average Log2FC > 0.5, FDR < 0.05, and pct. > 10%, three identified targets showed evidence of cell-type-specific enrichment in AKI renal tissues (**C**), while four targets exhibited enrichment in normal tissues (**D**). (**E**, **F**) Immune cells are divided into three cell types. (**G**, **H**, **I**) Comparison of TNFRSF1B expression levels in the three cell types

(*P.adj* < 0.05 and|log2FC| > 1), including CD-PC, DCT, Endo, LOH, and PT, suggesting a potential key role for *LTF* in the pathogenesis of AKI (Figure S5).

Furthermore, several genes exhibited cell type specificity. In AKI tissues, three druggable genes had cell-type-specific enrichment at average log2(FC) > 0.5, FDR < 0.05, and pct. > 10% level: *FAM3B* was enriched in CD-PC; *LTF* and *BRD9* were enriched in PT (Fig. 6C). In normal tissues, four druggable genes had cell-type-specific enrichment at the same level: *FAM3B* was enriched in CD-PC and CD-IC; *TNFRSF1B* was enriched in immune cells and Endo; *ADD1* was enriched in Endo; *ESR2* was enriched in RPC and PT (Fig. 6D). We further classified the immune cells and observed that *TNFRSF1B* was significantly more highly expressed in monocytes and T cells compared with B cells (Fig. 6E-I).

Mouse knock-out models for druggable genes

Models involving *NCF1*, *BRD9*, *ESR2*, *CDKN2C*, and *HSD17B3* displayed phenotypes such as kidney cysts, renal carcinoma, cortical renal glomerulopathy, abnormal kidney morphology, and abnormal urinary bladder morphology, suggesting an intrinsic role in the regulation of renal function (Table S7).

Drug repurposing and molecular docking

Searching DrugBank and ChEMBL databases, these druggable genes or proteins were identified as targets for 91 unique drugs that have been approved or are under investigation. Of these, spironolactone (targeting *ESR2*) is in Phase III clinical trials for the prevention of AKI, and arginine (targeting *ADC*) has been approved for the prevention of kidney injury. Other drugs are approved for the prevention or treatment of tumours, nutritional deficiencies, psychiatric disorders, menopause, and various other conditions. Detailed information on these drugs is summarized in Table S8.

To discover more promising drugs, we can use MR results to infer the type of pharmacological action needed to treat AKI and compare it to the action type of existing drugs. We prioritized the targets of tier 1 and tier 2 as the potential drug targets, and selected FDA-approved drug with a corresponding effect in the same direction as the SMR findings. Through this process, we observed two drug-target relationship matches: Dextromethorphan-*NCF1* and Tasonermin-*TNFRSF1B*. We also broadened the scope of potential drugs by querying CTD for the impact of pharmacological interventions on protein levels and gene expression levels. The promising drug-target relationships were shown in Table 3.

To determine the binding affinity between these small-molecule drugs and potential targets, we conducted molecular docking. To better contextualize binding affinities, we docked a clinically relevant AKI drug (Theophylline) as a positive control (Figure S6) [52]. All the valid docking results are presented in Fig. 7, among which, telmisartan-*NCF1* (-9.72 kcal/mol), calcitriol-*ACADSB* (-8.15 kcal/mol), and ethinyl estradiol-*ACADSB* (-8.87 kcal/mol) exhibited the lowest total binding free energies, indicating extremely stable interactions. Notably, ethinyl estradiol, acetaminophen, valproic acid, and propylthiouracil simultaneously target two or more significant AKI targets, with ethinyl estradiol exhibiting a high binding affinity for nearly all significant targets (Table 3). To validate the reliability of our docking protocol, we calculated the root-mean-square deviation (RMSD) between the predicted binding poses of known inhibitors and their experimentally determined structures using PyMOL 2.5. The RMSD values were less than 2 Å, confirming the accuracy of our docking approach.

Protein interaction and enrichment analysis with experimental drug targets

Through ClinicalTrials.gov, we identified 47 promising drugs undergoing AKI clinical trials corresponding to 92 unique targets (Table S9). Utilizing the STRING database and Cytoscape software, we constructed a PPI network comprising 19 candidate targets and 92 experimental drug targets for AKI (Fig. 8A, B). *NCF1* and *ESR2* demonstrated strong interactions with the targets of existing drugs (Fig. 8C). We then conducted Gene Ontology (GO) and Kyoto Encyclopedia of Genes and Genomes (KEGG) enrichment analyses based on these targets, with the top enriched biological pathways presented in Fig. 8D, E. Furthermore, several candidate targets (e.g., *NCF1*, *TNFRSF1B*, and *ADD1*) were significantly enriched with existing targets in pathways such as positive regulation of the MAPK cascade, regulation of muscle system processes, endothelium development, regulation of inflammatory response, and cellular response to inorganic substances (Table S10).

Discussion

Developing novel drugs for AKI poses significant challenges due to its complex pathophysiological mechanisms. Based on druggable pQTLs and eQTLs, we identified 19 causal biomarkers (seven proteins and twelve genes) for AKI. These proteins and genes were classified into three tiers based on MR, SMR and colocalization evidence. We further verified whether these biomarkers have any tissue-specific or cell-type-specific expression. Subsequently, we assessed the potential for drug-repurposing and conducted molecular docking. Some promising drugs were proposed, which need to be further investigated. Finally, a PPI network and enrichment analyses were conducted to investigate the interactions of the identified targets with existing targets and their biological significance.

Table 3 Molecular Docking results for potential drugs

Target	Drug Name	Druggability	Action Type	binding energy (kcal/mol)	RMSD (Å)	Tier
TNFRSF1B	Theophylline	Approved	Background	-3.92	0.001	1
	Estradiol	Approved	increased expression	-5.61	0.319	
	Ethinyl Estradiol	Approved	increased expression	-5.28	0.350	
	Fenretinide	Approved	increased expression	-5.10	1.509	
	Acetaminophen	Approved	increased expression	-3.09	1.070	
	Valproic Acid	Approved	increased expression	-3.10	1.577	
	Ketoconazole	Approved	increased expression	-2.82	1.224	
	Decitabine	Approved	increased expression	-3.33	0.479	
	Hydroquinone	Approved	increased expression	-2.81	3.242	
	Menthol	Approved	increased expression	-3.54	1.779	
	Mitotane	Approved	increased expression	-4.07	0.492	
	Mycophenolic Acid	Approved	increased expression	-2.03	0.855	
	Obeticholic Acid	Approved	increased expression	-3.56	1.297	
	Pioglitazone	Approved	increased expression	-3.19	1.358	
	Propylthiouracil	Approved	increased expression	-3.01	0.825	
	Streptozocin	Approved	increased expression	-1.64	2.009	
	Zoledronic Acid	Approved	increased expression	-0.51	2.791	
NCF1	Theophylline	Approved	Background	-4.06	0.000	1
	Dextromethorphan	Approved	Inhibitor	-6.09	0.000	
	Telmisartan	Approved	decreased expression	-9.72	0.153	
	Aspirin	Approved	decreased expression	-6.46	1.533	
	Benazepril	Approved	decreased expression	-6.25	3.799	
	Eplerenone	Approved	decreased expression	-6.89	0.000	
	Ethinyl Estradiol	Approved	decreased expression	-6.38	0.464	
	Niacin	Approved	decreased expression	-5.67	0.000	
	Pitavastatin	Approved	decreased expression	-6.02	0.884	
	Trandolapril	Approved	decreased expression	-4.46	1.689	
	Miconazole	Approved	decreased expression	-4.89	1.006	
	Metformin	Approved	decreased expression	-4.14	0.773	
APEH	Theophylline	Approved	Background	-3.77	0.000	1
	Ethinyl Estradiol	Approved	increased expression	-6.90	0.441	
	Methimazole	Approved	increased expression	-2.96	2.176	
	Propylthiouracil	Approved	increased expression	-4.15	0.780	
	Sulfadimethoxine	Approved	increased expression	-4.74	0.693	
ACADSB	Theophylline	Approved	Background	-4.41	0.000	2
	Acetaminophen	Approved	increased expression	-5.04	1.039	
	Belinostat	Approved	increased expression	-7.68	1.548	
	Calcitriol	Approved	increased expression	-8.15	0.289	
	Ethinyl Estradiol	Approved	increased expression	-8.87	0.000	
	Rosiglitazone	Approved	increased expression	-7.25	1.822	
	Tetracycline	Approved	increased expression	-7.16	0.000	
	Topiramate	Approved	increased expression	-6.64	0.671	
	Zidovudine	Approved	increased expression	-5.58	0.436	
	Valproic Acid	Approved	increased expression	-3.85	1.497	
	Lamivudine	Approved	increased expression	-4.95	1.326	
FAM3B	Theophylline	Approved	Background	-3.68	0.001	2
	Acetaminophen	Approved	decreased expression	-3.44	1.004	
	Azathioprine	Approved	decreased expression	-3.14	1.232	
	Urethane	Approved	decreased expression	-2.56	0.477	
ADD1	Theophylline	Approved	Background	-3.77	0.000	2
	Finasteride	Approved	increased expression	-5.20	1.683	
	Testosterone	Approved	increased expression	-5.01	3.131	
	Ethinyl Estradiol	Approved	increased expression	-5.28	0.472	

Table 3 (continued)

Target	Drug Name	Druggability	Action Type	binding energy (kcal/mol)	RMSD (Å)	Tier
	Coumarin	Approved	increased expression	-4.29	0.375	
	Acetaminophen	Approved	increased expression	-3.77	0.982	
	Tretinoin	Approved	increased expression	-4.25	0.997	
	Flutamide	Approved	increased expression	-3.44	1.496	
	Methotrexate	Approved	increased expression	-1.93	1.865	
	Nefazodone	Approved	increased expression	-2.54	2.303	
	Nimesulide	Approved	increased expression	-3.46	1.705	
	Sulindac	Approved	increased expression	-4.15	1.068	

NCF1, a regulatory subunit essential for activating latent NADPH oxidase, primarily *NOX2*, in the kidney to mediate the production of reactive oxygen species (ROS) [53]. Upregulation of *NOX2* abundance and *NCF1* expression is observed in various animal models of AKI and is accompanied by tissue damage due to excess ROS production and oxidative stress [54, 55]. Deletion of the *NCF1* gene effectively reduced ROS levels and attenuated oxidative stress in kidney-injured mice, significantly ameliorating adverse outcomes such as albuminuria and renal fibrosis, and reducing the risk of AKI [56, 57]. The AKI-promoting effect of *NCF1* was supported by the top tier of evidence in our study. Along with another tier 1 target, *TNFRSF1B*, involved in the regulation of inflammatory response pathway, a key component in the pathogenesis of AKI [12]. Furthermore, *NCF1* exhibited robust interactions with experimental AKI drug targets in the PPI network, suggesting that it could be a promising therapeutic target.

APEH and *TNFRSF1B* are two other tier 1 targets. *APEH*, a serine peptidase belonging to the prolyl oligopeptidase family, plays a crucial role in protein metabolism by catalyzing the hydrolysis of N-acetylated peptides and proteins [58]. Emerging evidence suggests that it may play a protective role in mitigating oxidative stress. *APEH* can degrade oxidatively damaged proteins [59, 60], and reduced *APEH* activity has been detected in diseases associated with inflammation, oxidative stress, lipid peroxidation, and oxidative damage, such as type 2 diabetes and Alzheimer's disease [61, 62]. Aberrant expression of *APEH* has also been observed in AKI, and in the present study, lower expression levels of *APEH* were associated with an increased risk of AKI. *TNFRSF1B*, also known as *TNFR2*, is a member of the tumor necrosis factor (*TNF*) receptor superfamily. *TNFRSF1B* is primarily expressed in endothelial cells and immune cells, where it plays a role in cell survival [63]. Studies have shown that the interaction between *TNFα* and *TNFRSF1B* inhibits ischemia-reperfusion injury [64], a significant risk factor for AKI [65]. Additionally, *TNFRSF1B* mediates the activating effect of *TNFα* on regulatory T (Treg) cells [66], which helps reduce the risk of ischemic AKI and aids in injury repair [67, 68]. Notably, up-regulation of the expression level of *TNFRSF1B* was observed in AKI tissues, which may be a sign that *TNFRSF1B* achieves its protective effect against AKI by suppressing excessive immune response or inhibiting inflammatory response [69].

The remaining druggable genes could provide further insights into the discovery of drug targets. *ACADSB* functions to catalyze the initial step in each cycle of fatty acid (FA) β-oxidation in mitochondria [70]. As the primary site of injury in AKI, the proximal tubule has high energy demand, and FA β-oxidation is its most efficient mechanism for producing ATP [71]. A decrease in *ACADSB* expression level can lead to impaired FA β-oxidation and a reduction in ATP production [72]. Furthermore, the reduction of FA β-oxidation can cause intrarenal lipid accumulation, inducing lipotoxicity and impairing renal function [73], which is associated with AKI in numerous animal experimental [74, 75]. Studies have shown that *ADD1* polymorphisms were associated with decreased renal plasma flow [76], decreased glomerular filtration rate [76], increased urinary protein [77], and poor prognosis in IgA nephropathy [78]. In addition, *ADD1* phosphorylation is increased in cisplatin-induced apoptosis of renal proximal tubular epithelial cells [79]. *FAM3B* is considered a promising therapeutic target for non-alcoholic fatty liver disease and type 2 diabetes mellitus [80]. However, the role of *FAM3B* in the kidney is poorly studied. In our study, *FAM3B* was found to be enriched in CD-PC, with higher protein levels correlating with an increased risk of developing AKI. It has been shown that knockdown of *ESR2* inhibits ketone body production and exacerbate ischemic AKI [81]. Frehmaglutinin D and rehmaionoside C can ameliorate LPS-induced acute kidney injury in vivo and in vitro via the *ESR2*-mediated TLR4 pathway [82]. *LTF* may exert nephroprotective effects in glycerol-induced AKI or chromium-induced AKI via anti-inflammatory and antioxidant pathways [83, 84]. In addition, a multi-ancestry proteome-wide MR study implicates that higher genetically predicted concentration of *TCN2* was associated with a higher estimated glomerular filtration rate [85]. Predictive models using *CD244* as one of the frameworks have been used to predict the risk of AKI after cardiac surgery [86]. In

Code	Drug-target relationships	binding energy (kcal/mol)
a	Dextromethorphan-*NCF1*	-6.09
b	Telmisartan-*NCF1*	-9.72
c	Aspirin-*NCF1*	-6.46
d	Benazepril-*NCF1*	-6.25
e	Eplerenone-*NCF1*	-6.89
f	Ethinyl Estradiol-*NCF1*	-6.38
g	Niacin-*NCF1*	-5.67
h	Pitavastatin-*NCF1*	-6.02
i	Ethinyl Estradiol-*APEH*	-6.90
j	Estradiol-*TNFRSF1B*	-5.61
k	Ethinyl Estradiol-*TNFRSF1B*	-5.28
l	Fenretinide-*TNFRSF1B*	-5.10

Code	Drug-target relationships	binding energy (kcal/mol)
m	Acetaminophen-*ACADSB*	-5.04
n	Belinostat-*ACADSB*	-7.68
o	Calcitriol-*ACADSB*	-8.15
p	Ethinyl Estradiol-*ACADSB*	-8.87
q	Rosiglitazone-*ACADSB*	-7.25
r	Tetracycline-*ACADSB*	-7.16
s	Topiramate-*ACADSB*	-6.64
t	Zidovudine-*ACADSB*	-5.58
u	Finasteride-*ADD1*	-5.20
v	Testosterone-*ADD1*	-5.01
w	Ethinyl Estradiol-*ADD1*	-5.28

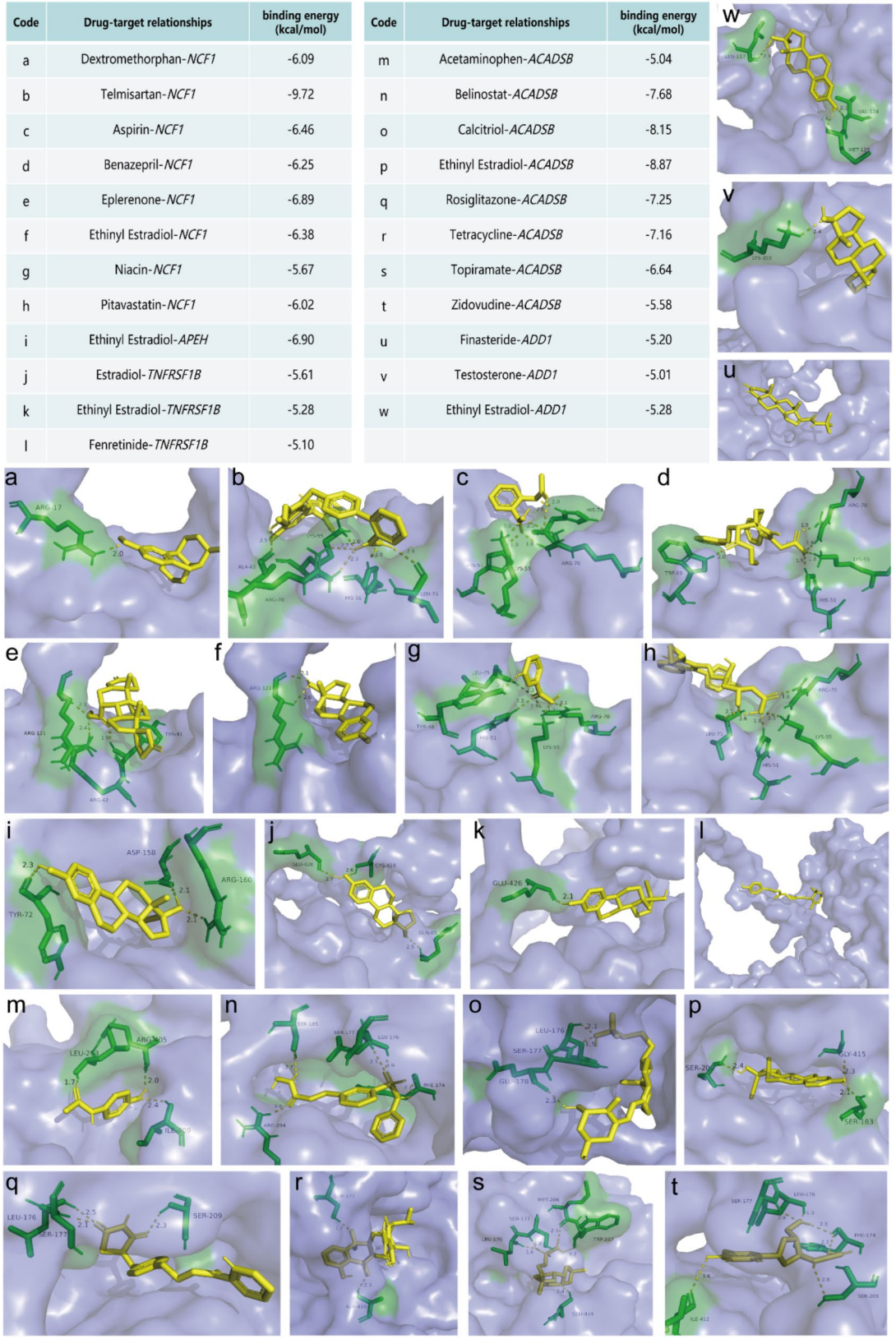

Fig. 7 Molecular docking results for potential drugs. *Drug docking results that exhibit high binding affinity to candidate targets (binding energy <-5 kcal/mol)*

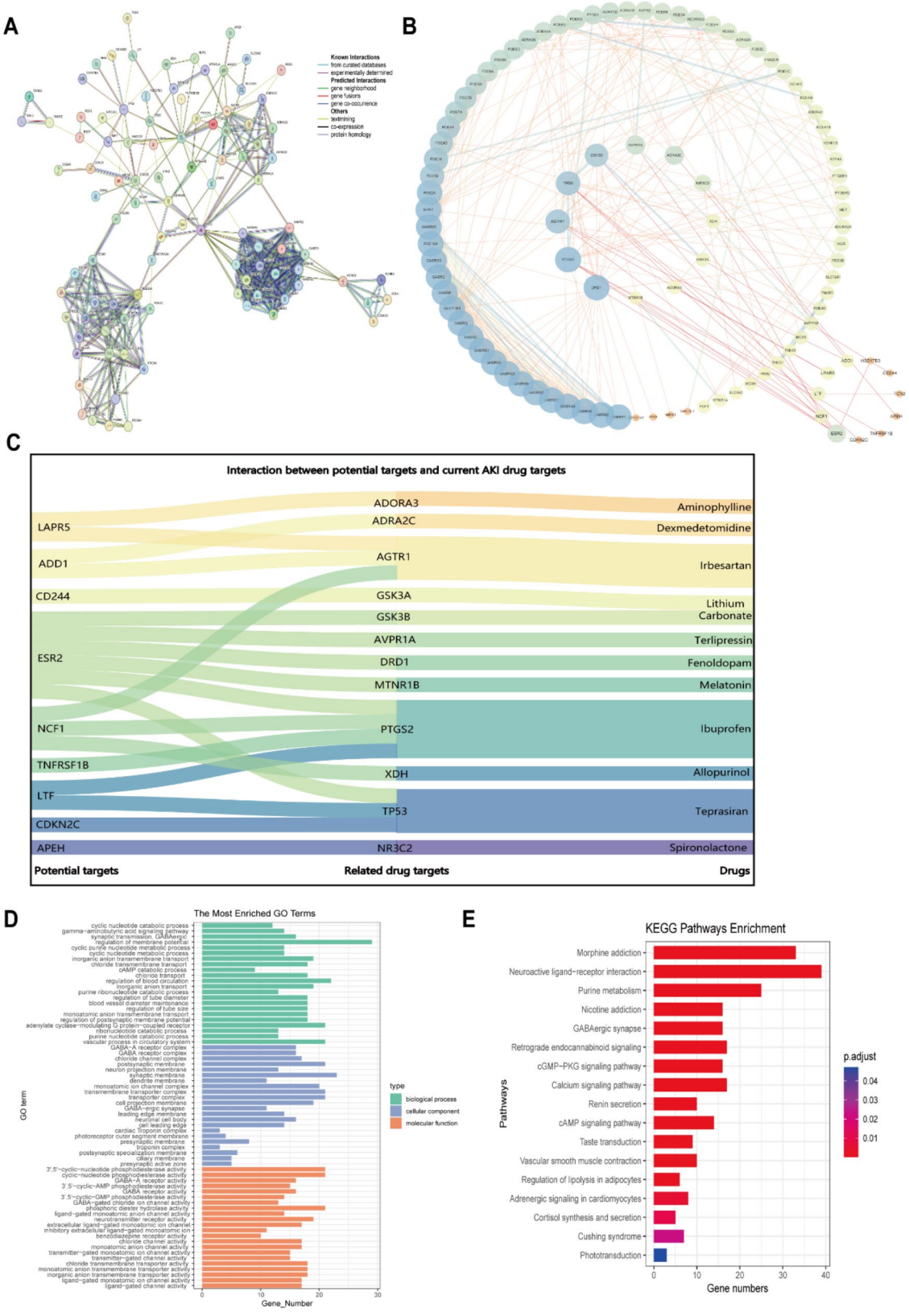

Fig. 8 (See legend on next page.)

(See figure on previous page.)

Fig. 8 Target-drug-target association networks and enrichment analysis. (**A**) Protein-protein interaction network of 19 candidate targets and 92 experimental AKI drug targets using the STRING database. (**B**) PPI network mapped using Cytoscape software. Small circles represent candidate targets identified in this study, medium circles denote experimental AKI drug targets associated with the candidate targets, and large circles indicate drug targets without such associations. Edges represent protein-protein interactions retrieved from the STRING database (confidence score > 0.7). The size of each node corresponds to its degree of connectivity, with larger nodes indicating more interactions. (**C**) Association between candidate targets and experimental AKI drug targets. Using the Sankey diagram, we mapped a "candidate target-experimental drug target-experimental drug" network. (**D**, **E**) GO and KEGG enrichment analysis (only the most significant pathways are shown)

conclusion, multiple previous studies support the drug targets identified in our study.

Regarding drug-repurposing, we prioritized tier 1 and tier 2 targets for evaluation. We incorporated approved drugs corresponding to these targets, thereby ensuring a robust safety profile. The high binding activity of molecular docking indicates the great potential of these targets. Indeed, numerous drugs identified through molecular docking have shown protective effects in various types of AKI, including telmisartan [87], aspirin [88], benadryl [89], eplerenone [90], pitavastatin [91], estradiol [92], acetaminophen [93], calcitriol [94], rosiglitazone [95], and testosterone [96]. Some drugs that act on multiple targets or pathways simultaneously may perform better in the treatment of AKI. Some tier 3 targets, although not supported by SMR and colocalization for various reasons, still deserve attention. For example, the drug targeting *ESR2*, spironolactone, is in Phase III trials for AKI. Additionally, we further constructed a PPI network and a "candidate target-experimental drug target-experimental drug" association network containing the 19 candidate targets of this study and the 92 experimental drug targets. Since candidate targets do not act independently but rather in combination with a complex network of interrelated pathways that determine disease progression [97], when the candidate targets in this study is not available, other proteins in the shared pathway may also provide therapeutic options. Moreover, interlinking the novel targets identified in this study with known targets may also provide new insights for combination therapy involving multiple targets.

Notably, in this study, we augmented the confidence of our identified druggable targets with several sensitivity analyses. In our colocalization analysis, we applied prior probabilities (p1, $p2 = 1 \times 10^{-4}$), which are commonly used in similar studies and are the default settings in the coloc R package [24, 25, 98]. To assess the robustness of our findings, we performed a sensitivity analysis by varying the prior probabilities (p1, p2) across a range of values (1×10^{-3} to 1×10^{-5}). As summarized in Table S5, we observed that the posterior probability for colocalization (PP4) remained stable regardless of the prior settings, indicating that our findings are largely driven by the observed association signals rather than the choice of prior probabilities. This result is consistent with previous studies [99], where strong signal overlap renders variations in prior probabilities negligible in colocalization analyses. These findings further support the robustness of our colocalization results and confirm that the identified colocalized loci are unlikely to be artifacts of prior selection.

For Mendelian randomization, we applied a 1,000 kb cis-window to select instrumental variables, which is a commonly used threshold in pQTL/eQTL-based MR analyses [25, 98, 100]. This window size ensures the inclusion of potentially regulatory genetic variants that may affect gene expression or protein levels within cis-regulatory regions while balancing the risk of linkage disequilibrium (LD) contamination. Some studies have used stricter thresholds (e.g., 500 kb or 250 kb) to minimize the inclusion of variants that may be in LD with but not causally related to the exposure gene [101, 102]. However, evidence suggests that regulatory elements and enhancer-promoter interactions may extend beyond 500 kb in some contexts, particularly for genes with complex regulatory landscapes [103]. Thus, overly restrictive cis-windows could lead to the exclusion of valid instruments, potentially limiting statistical power.

To ensure independence among instrumental variables, we applied an LD pruning window of 10 Mb, which aligns with the default setting in PLINK, a widely used tool for LD-based SNP clumping [104–106]. This threshold is frequently used in GWAS and MR studies to remove SNPs in high LD while preserving the most strongly associated independent variants. Although some MR studies have employed smaller pruning windows (250 kb – 1,000 kb) to minimize LD confounding, overly restrictive thresholds may result in the exclusion of valid weak instruments, reducing statistical power [107]. To assess the impact of LD pruning choices, we performed sensitivity analyses using alternative pruning windows (500 kb) and compared MR estimates across different settings. The results demonstrated that 83.3% of eQTL targets and 85.7% of pQTL targets remained statistically significant, with effect directions fully consistent with our original findings (Table S6). These results confirm that our instrument selection approach is robust to variations in LD pruning settings and that LD-related confounding does not significantly impact our core conclusions.

To our knowledge, this is the first MR study on QTLs and AKI outcomes, with several strengths as outlined below. First, we integrated druggable eQTLs and pQTLs with the largest AKI GWAS to perform systematic proteome-wide and transcriptome-wide analysis. Second,

by integrating evidence of colocalization, transcript-level validation, protein interactions, and pathway enrichment, insights into the potential roles of these proteins and genes were obtained from various perspectives. Third, we identified some approved drugs with repurposing potential that have already passed fundamental stages of drug discovery, development, and clinical trials, offering significant time and cost advantages over novel drug-development. Some limitations should also be noted. First, the limited number of pQTLs and eQTLs meant that many proteins or genes were excluded from the analysis, restricting the identification of additional candidate targets and validation of those identified. Second, although database queries and molecular docking offer suggestive evidence for identifying potential drugs, they cannot ensure the effectiveness of these candidates in clinical settings. Third, due to the lack of relevant biological data, this study did not conduct an analysis of the various AKI subtypes. Last, our study used the Ferkingstad et al. pQTL dataset, which is derived exclusively from an Icelandic population. Its generalizability to other populations may be limited due to differences in allele frequencies, LD structures, and genetic diversity. These population-specific characteristics could introduce bias in the selection of instrumental variables and the interpretation of colocalization results, potentially affecting the robustness of our findings. To address this limitation, future studies should aim to replicate our analyses in more genetically diverse populations, which would help assess the applicability of our conclusions across different genetic backgrounds and enhance the generalizability of the results.

Conclusions

In conclusion, our systematic proteome-wide and transcriptome-wide analyses identified seven proteins and twelve genes as potential therapeutic targets for AKI. Follow-up analyses also proposed several promising drugs for further investigation. Future research should focus on larger studies across diverse AKI subtypes and populations with different genetic backgrounds, as well as in-depth mechanistic studies to validate our findings and elucidate the underlying biological pathways.

Supplementary Information

The online version contains supplementary material available at https://doi.org/10.1186/s13062-025-00631-0.

Supplementary Material 1

Supplementary Material 2

Acknowledgements
The authors thank all investigators and participants for providing the GWAS data and transcript-level data mentioned in the article. This work was made possible by the generous sharing of statistics from the public databases.

Author contributions
JL and DZ conceptualized and designed the study. YW, FD, and ZD contributed to the study design and data acquisition. JL, DZ, and ZD contributed to data interpretation and manuscript revision. JL and DZ conducted the statistical analyses and drafted the manuscript. SW contributed to the revision process, including additional sensitivity analyses and technical refinements. All authors have reviewed and approved the final manuscript. ZD and SW will serve as the corresponding authors for future inquiries regarding this study.

Funding
This work is supported by the Natural Science Foundation of Hunan Province, China (No. 2023JJ40861).

Data availability
All data generated or analyzed during this study are included in this published article and its supplementary information files. The datasets used and/or analysed during the current study are available from the corresponding author on reasonable request.

Declarations

Ethics approval and consent to participate
The data collected in this study came from FinnGen Consortium and other public databases; the data were desensitized before uploading and did not involve personal privacy or identifiable information. This study did not involve information and data and informed consent authorization of the institution, so no ethical review was not necessary.

Consent for publication
Not applicable.

Competing interests
The authors declare no competing interests.

Author details
[1]Department of Urology, The Second Xiangya Hospital at Central South University, Changsha 410011, Hunan, China
[2]Xiangya Hospital, Central South University, Changsha, Hunan, China
[3]Department of Nephrology, The Second Xiangya Hospital, Central South University, Changsha, Hunan, China
[4]Xiangya School of Medicine, Central South University, Changsha, Hunan, China

Received: 28 January 2025 / Accepted: 11 March 2025
Published online: 27 March 2025

References

1. Kellum JA, Romagnani P, Ashuntantang G, Ronco C, Zarbock A, Anders HJ. Acute kidney injury. Nat Rev Dis Primers. 2021;7(1):52.
2. Susantitaphong P, Cruz DN, Cerda J, Abulfaraj M, Alqahtani F, Koulouridis I, et al. World incidence of AKI: a meta-analysis. Clin J Am Soc Nephrol. 2013;8(9):1482–93.
3. Sohaney R, Yin H, Shahinian V, Saran R, Burrows NR, Pavkov ME, et al. In-Hospital and 1-Year mortality trends in a National cohort of US veterans with acute kidney injury. Clin J Am Soc Nephrol. 2022;17(2):184–93.
4. Lunyera J, Clare RM, Chiswell K, Scialla JJ, Pun PH, Thomas KL, et al. Association of acute kidney injury and cardiovascular disease following percutaneous coronary intervention: assessment of interactions by race, diabetes, and kidney function. Am J Kidney Dis. 2023;81(6):707–16.
5. Ikizler TA, Parikh CR, Himmelfarb J, Chinchilli VM, Liu KD, Coca SG, et al. A prospective cohort study of acute kidney injury and kidney outcomes, cardiovascular events, and death. Kidney Int. 2021;99(2):456–65.
6. Rydén L, Sartipy U, Evans M, Holzmann MJ. Acute kidney injury after coronary artery bypass grafting and long-term risk of end-stage renal disease. Circulation. 2014;130(23):2005–11.
7. Mercado MG, Smith DK, Guard EL. Acute kidney injury: diagnosis and management. Am Fam Physician. 2019;100(11):687–94.

8. Kellum JA, Lameire N, Aspelin P, Barsoum RS, Burdmann EA, Goldstein SL, et al. Kidney disease: improving global outcomes (KDIGO) acute kidney injury work group. KDIGO clinical practice guideline for acute kidney injury. Kidney Int Supplements. 2012;2(1):1–138.
9. Wald R, Beaubien-Souligny W, Chanchlani R, Clark EG, Neyra JA, Ostermann M, et al. Delivering optimal renal replacement therapy to critically ill patients with acute kidney injury. Intensive Care Med. 2022;48(10):1368–81.
10. Ronco C, Bellomo R, Kellum JA. Acute kidney injury. Lancet. 2019;394(10212):1949–64.
11. Aranda-Rivera AK, Cruz-Gregorio A, Aparicio-Trejo OE, Pedraza-Chaverri J. Mitochondrial redox signaling and oxidative stress in kidney diseases. Biomolecules. 2021;11:8.
12. Chen J, Wang W, Tang Y, Huang XR, Yu X, Lan HY. Inflammatory stress in SARS-COV-2 associated acute kidney injury. Int J Biol Sci. 2021;17(6):1497–506.
13. Maremonti F, Meyer C, Linkermann A. Mechanisms and models of kidney tubular necrosis and nephron loss. J Am Soc Nephrol. 2022;33(3):472–86.
14. Qu L, Jiao B. The interplay between immune and metabolic pathways in kidney disease. Cells. 2023;12(12).
15. Xu Y, Zou P, Cao X. Advances in pharmacotherapy for acute kidney injury. Expert Opin Pharmacother. 2022;23(6):713–26.
16. Hoste EAJ, Kellum JA, Selby NM, Zarbock A, Palevsky PM, Bagshaw SM, et al. Global epidemiology and outcomes of acute kidney injury. Nat Rev Nephrol. 2018;14(10):607–25.
17. Ho D, Quake SR, McCabe ERB, Chng WJ, Chow EK, Ding X, et al. Enabling technologies for personalized and precision medicine. Trends Biotechnol. 2020;38(5):497–518.
18. Nourie N, Ghaleb R, Lefaucheur C, Louis K. Toward precision medicine: exploring the landscape of biomarkers in acute kidney injury. Biomolecules. 2024;14(1).
19. Ortega-Loubon C, Martínez-Paz P, García-Morán E, Tamayo-Velasco Á, López-Hernández FJ, Jorge-Monjas P et al. Genetic susceptibility to acute kidney injury. J Clin Med. 2021;10(14).
20. Zhao B, Lu Q, Cheng Y, Belcher JM, Siew ED, Leaf DE, et al. A Genome-Wide association study to identify Single-Nucleotide polymorphisms for acute kidney injury. Am J Respir Crit Care Med. 2017;195(4):482–90.
21. Stafford-Smith M, Li YJ, Mathew JP, Li YW, Ji Y, Phillips-Bute BG, et al. Genome-wide association study of acute kidney injury after coronary bypass graft surgery identifies susceptibility loci. Kidney Int. 2015;88(4):823–32.
22. Finan C, Gaulton A, Kruger FA, Lumbers RT, Shah T, Engmann J et al. The drug-gable genome and support for target identification and validation in drug development. Sci Transl Med. 2017;9(383).
23. Sekula P, Del Greco MF, Pattaro C, Köttgen A. Mendelian randomization as an approach to assess causality using observational data. J Am Soc Nephrol. 2016;27(11):3253–65.
24. Chen J, Xu F, Ruan X, Sun J, Zhang Y, Zhang H, et al. Therapeutic targets for inflammatory bowel disease: proteome-wide Mendelian randomization and colocalization analyses. EBioMedicine. 2023;89:104494.
25. Rasooly D, Peloso GM, Pereira AC, Dashti H, Giambartolomei C, Wheeler E, et al. Genome-wide association analysis and Mendelian randomization proteomics identify drug targets for heart failure. Nat Commun. 2023;14(1):3826.
26. Wang Y, Chen G, Li D. Integrated Mendelian randomization and single-cell RNA-sequencing analyses identified OAS1 as a novel therapeutic target for erectile dysfunction via targeting fibroblasts. Biol Direct. 2024;19(1):136.
27. Sakaue S, Kanai M, Tanigawa Y, Karjalainen J, Kurki M, Koshiba S, et al. A cross-population atlas of genetic associations for 220 human phenotypes. Nat Genet. 2021;53(10):1415–24.
28. Famulski KS, de Freitas DG, Kreepala C, Chang J, Sellares J, Sis B, et al. Molecular phenotypes of acute kidney injury in kidney transplants. J Am Soc Nephrol. 2012;23(5):948–58.
29. Janosevic D, Myslinski J, McCarthy T, Zollman A, Syed F, Xuei X et al. The orchestrated cellular and molecular responses of the kidney to endotoxin define the sepsis timeline. BioRxiv. 2020:2020.05.27.118620.
30. Tsalik EL, Willig LK, Rice BJ, van Velkinburgh JC, Mohney RP, McDunn JE, et al. Renal systems biology of patients with systemic inflammatory response syndrome. Kidney Int. 2015;88(4):804–14.
31. Legouis D, Rinaldi A, Malpetti D, Arnoux G, Verissimo T, Faivre A, et al. A transfer learning framework to elucidate the clinical relevance of altered proximal tubule cell States in kidney disease. iScience. 2024;27(3):109271.
32. Ferkingstad E, Sulem P, Atlason BA, Sveinbjornsson G, Magnusson MI, Styrmisdottir EL, et al. Large-scale integration of the plasma proteome with genetics and disease. Nat Genet. 2021;53(12):1712–21.
33. Võsa U, Claringbould A, Westra HJ, Bonder MJ, Deelen P, Zeng B, et al. Large-scale cis- and trans-eQTL analyses identify thousands of genetic loci and polygenic scores that regulate blood gene expression. Nat Genet. 2021;53(9):1300–10.
34. Skrivankova VW, Richmond RC, Woolf BAR, Yarmolinsky J, Davies NM, Swanson SA, et al. Strengthening the reporting of observational studies in epidemiology using Mendelian randomization: the STROBE-MR statement. JAMA. 2021;326(16):1614–21.
35. Sun BB, Maranville JC, Peters JE, Stacey D, Staley JR, Blackshaw J, et al. Genomic atlas of the human plasma proteome. Nature. 2018;558(7708):73–9.
36. Pierce BL, Ahsan H, Vanderweele TJ. Power and instrument strength requirements for Mendelian randomization studies using multiple genetic variants. Int J Epidemiol. 2011;40(3):740–52.
37. Hemani G, Bowden J, Davey Smith G. Evaluating the potential role of Pleiotropy in Mendelian randomization studies. Hum Mol Genet. 2018;27(R2):R195–208.
38. Bowden J, Davey Smith G, Burgess S. Mendelian randomization with invalid instruments: effect Estimation and bias detection through Egger regression. Int J Epidemiol. 2015;44(2):512–25.
39. Hemani G, Tilling K, Davey Smith G. Orienting the causal relationship between imprecisely measured traits using GWAS summary data. PLoS Genet. 2017;13(11):e1007081.
40. Verbanck M, Chen CY, Neale B, Do R. Detection of widespread horizontal Pleiotropy in causal relationships inferred from Mendelian randomization between complex traits and diseases. Nat Genet. 2018;50(5):693–8.
41. Giambartolomei C, Vukcevic D, Schadt EE, Franke L, Hingorani AD, Wallace C, et al. Bayesian test for colocalisation between pairs of genetic association studies using summary statistics. PLoS Genet. 2014;10(5):e1004383.
42. Zhu Z, Zhang F, Hu H, Bakshi A, Robinson MR, Powell JE, et al. Integration of summary data from GWAS and eQTL studies predicts complex trait gene targets. Nat Genet. 2016;48(5):481–7.
43. Ritchie ME, Phipson B, Wu D, Hu Y, Law CW, Shi W, et al. Limma powers differential expression analyses for RNA-sequencing and microarray studies. Nucleic Acids Res. 2015;43(7):e47.
44. Butler A, Hoffman P, Smibert P, Papalexi E, Satija R. Integrating single-cell transcriptomic data across different conditions, technologies, and species. Nat Biotechnol. 2018;36(5):411–20.
45. Korsunsky I, Millard N, Fan J, Slowikowski K, Zhang F, Wei K, et al. Fast, sensitive and accurate integration of single-cell data with harmony. Nat Methods. 2019;16(12):1289–96.
46. Knox C, Wilson M, Klinger CM, Franklin M, Oler E, Wilson A, et al. Drug-Bank 6.0: the drugbank knowledgebase for 2024. Nucleic Acids Res. 2024;52(D1):D1265–75.
47. Zdrazil B, Felix E, Hunter F, Manners EJ, Blackshaw J, Corbett S, et al. The chembl database in 2023: a drug discovery platform spanning multiple bioactivity data types and time periods. Nucleic Acids Res. 2024;52(D1):D1180–92.
48. Davis AP, Wiegers TC, Johnson RJ, Sciaky D, Wiegers J, Mattingly CJ. Comparative toxicogenomics database (CTD): update 2023. Nucleic Acids Res. 2023;51(D1):D1257–62.
49. Morris GM, Huey R, Lindstrom W, Sanner MF, Belew RK, Goodsell DS, et al. AutoDock4 and AutoDockTools4: automated Docking with selective receptor flexibility. J Comput Chem. 2009;30(16):2785–91.
50. Seeliger D, de Groot BL. Ligand Docking and binding site analysis with PyMOL and Autodock/Vina. J Comput Aided Mol Des. 2010;24(5):417–22.
51. Shannon P, Markiel A, Ozier O, Baliga NS, Wang JT, Ramage D, et al. Cytoscape: a software environment for integrated models of biomolecular interaction networks. Genome Res. 2003;13(11):2498–504.
52. Dai B, Liu Y, Fu L, Li Y, Zhang J, Mei C. Effect of Theophylline on prevention of contrast-induced acute kidney injury: a meta-analysis of randomized controlled trials. Am J Kidney Dis. 2012;60(3):360–70.
53. Sedeek M, Nasrallah R, Touyz RM, Hébert RL. NADPH oxidases, reactive oxygen species, and the kidney: friend and foe. J Am Soc Nephrol. 2013;24(10):1512–8.
54. Reel B, Guzeloglu M, Bagriyanik A, Atmaca S, Aykut K, Albayrak G, et al. The effects of PPAR-γ agonist Pioglitazone on renal ischemia/reperfusion injury in rats. J Surg Res. 2013;182(1):176–84.
55. Maddens B, Vandendriessche B, Demon D, Vanholder R, Chiers K, Cauwels A, et al. Severity of sepsis-induced acute kidney injury in a novel mouse model is age dependent. Crit Care Med. 2012;40(9):2638–46.

56. Liu GC, Fang F, Zhou J, Koulajian K, Yang S, Lam L, et al. Deletion of p47phox attenuates the progression of diabetic nephropathy and reduces the severity of diabetes in the Akita mouse. Diabetologia. 2012;55(9):2522–32.
57. Wang H, Chen X, Su Y, Paueksakon P, Hu W, Zhang MZ, et al. p47(phox) contributes to albuminuria and kidney fibrosis in mice. Kidney Int. 2015;87(5):948–62.
58. Polgár L. The Prolyl oligopeptidase family. Cell Mol Life Sci CMLS. 2002;59(2):349–62.
59. Yoshioka K, Komatsu T, Hanaoka K, Ueno T, Terai T, Nagano T, et al. Discovery of a pyruvylated peptide-metabolizing enzyme using a fluorescent substrate-based protein discovery technique. Chem Commun (Camb). 2016;52(23):4377–80.
60. Nakai A, Yamauchi Y, Sumi S, Tanaka K. Role of acylamino acid-releasing enzyme/oxidized protein hydrolase in sustaining homeostasis of the cytoplasmic antioxidative system. Planta. 2012;236(2):427–36.
61. Isaac M, Dustin P, Heidi J, Damien R, Matthew N, Tracy MC. Analyzing the activity and expression of acyl peptide enzyme hydrolase (APEH) in the blood serum of patients with type II diabetes. BIOS. 2019;90(2):70–8.
62. Palmieri G, Cocca E, Gogliettino M, Valentino R, Ruvo M, Cristofano G, et al. Low erythrocyte levels of proteasome and Acyl-Peptide hydrolase (APEH) activities in Alzheimer's disease: A sign of defective proteostasis?? J Alzheimers Dis. 2017;60(3):1097–106.
63. Faustman DL, Davis M. TNF receptor 2 and disease: autoimmunity and regenerative medicine. Front Immunol. 2013;4.
64. Kouyoumdjian A, Tchervenkov J, Paraskevas S. TFNR2 in Ischemia-Reperfusion injury, rejection, and tolerance in transplantation. Front Immunol. 2022;13:903913.
65. Liu W, Xiong Z, Fu T, Yang J, Zou J, Wu Y, et al. Regulation of renal ischemia-reperfusion injury and tubular epithelial cell ferroptosis by Ppary m6a methylation: mechanisms and therapeutic implications. Biol Direct. 2024;19(1):99.
66. Chen X, Oppenheim JJ. The phenotypic and functional consequences of tumour necrosis factor receptor type 2 expression on CD4(+) FoxP3(+) regulatory T cells. Immunology. 2011;133(4):426–33.
67. Gandolfo MT, Jang HR, Bagnasco SM, Ko GJ, Agreda P, Satpute SR, et al. Foxp3 + regulatory T cells participate in repair of ischemic acute kidney injury. Kidney Int. 2009;76(7):717–29.
68. Kinsey GR, Huang L, Vergis AL, Li L, Okusa MD. Regulatory T cells contribute to the protective effect of ischemic preconditioning in the kidney. Kidney Int. 2010;77(9):771–80.
69. Nguyen M-TJP, Fryml E, Sahakian SK, Liu S, Cantarovich M, Lipman M, et al. Pretransplant recipient Circulating CD4 + CD127lo/– tumor necrosis factor receptor 2 + regulatory T cells: A surrogate of regulatory T Cell–Suppressive function and predictor of delayed and slow graft function after kidney transplantation. Transplantation. 2016;100(2):314–24.
70. Thorpe C, Kim JJ. Structure and mechanism of action of the acyl-CoA dehydrogenases. Faseb J. 1995;9(9):718–25.
71. Bhargava P, Schnellmann RG. Mitochondrial energetics in the kidney. Nat Rev Nephrol. 2017;13(10):629–46.
72. Jiang P, Iqbal A, Wang M, Li X, Fang X, Yu H, et al. Transcriptomic analysis of Short/Branched-Chain Acyl-Coenzyme a dehydrogenase knocked out bMECs revealed its regulatory effect on lipid metabolism. Front Vet Sci. 2021;8:744287.
73. Bobulescu IA. Renal lipid metabolism and lipotoxicity. Curr Opin Nephrol Hypertens. 2010;19(4):393–402.
74. Portilla D, Li S, Nagothu KK, Megyesi J, Kaissling B, Schnackenberg L, et al. Metabolomic study of cisplatin-induced nephrotoxicity. Kidney Int. 2006;69(12):2194–204.
75. Zager RA, Johnson AC, Hanson SY. Renal tubular triglyercide accumulation following endotoxic, toxic, and ischemic injury. Kidney Int. 2005;67(1):111–21.
76. Beeks E, van der Klauw MM, Kroon AA, Spiering W, Fuss-Lejeune MJ, de Leeuw PW. Alpha-adducin Gly460Trp polymorphism and renal hemodynamics in essential hypertension. Hypertension. 2004;44(4):419–23.
77. Ferrandi M, Cusi D, Molinari I, Del Vecchio L, Barlassina C, Rastaldi MP, et al. alpha- and beta-Adducin polymorphisms affect podocyte proteins and proteinuria in rodents and decline of renal function in human IgA nephropathy. J Mol Med (Berl). 2010;88(2):203–17.
78. Narita I, Goto S, Saito N, Song J, Ajiro J, Sato F, et al. Interaction between ACE and ADD1 gene polymorphisms in the progression of IgA nephropathy in Japanese patients. Hypertension. 2003;42(3):304–9.
79. van de Water B, Tijdens IB, Verbrugge A, Huigsloot M, Dihal AA, Stevens JL, et al. Cleavage of the actin-capping protein alpha -adducin at Asp-Asp-Ser-Asp633-Ala by caspase-3 is preceded by its phosphorylation on Serine 726 in cisplatin-induced apoptosis of renal epithelial cells. J Biol Chem. 2000;275(33):25805–13.
80. Zhang X, Yang W, Wang J, Meng Y, Guan Y, Yang J. FAM3 gene family: A promising therapeutical target for NAFLD and type 2 diabetes. Metabolism. 2018;81:71–82.
81. Gui Y, Palanza Z, Gupta P, Li H, Pan Y, Wang Y et al. Calponin 2 regulates ketogenesis to mitigate acute kidney injury. JCI Insight. 2023;8(21).
82. Liu M, Guo P, Zeng M, Zhang Y, Jia J, Liu Y, et al. Effects and mechanisms of frehmaglutin D and Rehmaionoside C improve LPS-induced acute kidney injury through the Estrogen receptor-mediated TLR4 pathway in vivo and in vitro. Phytomedicine. 2024;123:155218.
83. Madkour AH, Helal MG, Said E, Salem HA. Dose-dependent renoprotective impact of lactoferrin against glycerol-induced rhabdomyolysis and acute kidney injury. Life Sci. 2022;302:120646.
84. Hegazy R, Salama A, Mansour D, Hassan A. Renoprotective effect of lactoferrin against Chromium-Induced acute kidney injury in rats: involvement of IL-18 and IGF-1 Inhibition. PLoS ONE. 2016;11(3):e0151486.
85. Lanktree MB, Perrot N, Smyth A, Chong M, Narula S, Shanmuganathan M, et al. A novel multi-ancestry proteome-wide Mendelian randomization study implicates extracellular proteins, tubular cells, and fibroblasts in estimated glomerular filtration rate regulation. Kidney Int. 2023;104(6):1170–84.
86. Entwistle A, Walker S, Knecht A, Strum SL, Shah A, Podgoreanu MV et al. A signature of pre-operative biomarkers of cellular senescence to predict risk of cardiac and kidney adverse events after cardiac surgery. MedRxiv. 2023.
87. Kocak C, Kocak FE, Akcilar R, Bayat Z, Aras B, Metineren MH, et al. Effects of Captopril, Telmisartan and Bardoxolone Methyl (CDDO-Me) in ischemia-reperfusion-induced acute kidney injury in rats: an experimental comparative study. Clin Exp Pharmacol Physiol. 2016;43(2):230–41.
88. Tong D, Xu E, Ge R, Hu M, Jin S, Mu J, et al. Aspirin alleviates cisplatin-induced acute kidney injury through the AMPK-PGC-1α signaling pathway. Chem Biol Interact. 2023;380:110536.
89. Li XM, Cong HL, Li TT, He LJ, Zhou YJ. Impact of Benazepril on contrast-induced acute kidney injury for patients with mild to moderate renal insufficiency undergoing percutaneous coronary intervention. Chin Med J (Engl). 2011;124(14):2101–6.
90. Barati A, Rahbar Saadat Y, Meybodi SM, Nouraei S, Moradi K, Kamrani Moghaddam F, et al. Eplerenone reduces renal ischaemia/reperfusion injury by modulating Klotho, NF-κB and SIRT1/SIRT3/PGC-1α signalling pathways. J Pharm Pharmacol. 2023;75(6):819–27.
91. Kaushik S, Tomar A, Puthanmadhom Narayanan S, Nag TC, Arya DS, Bhatia J. Pitavastatin attenuates cisplatin-induced renal injury by targeting MAPK and apoptotic pathways. J Pharm Pharmacol. 2019;71(7):1072–81.
92. Andrianova NV, Brezgunova AA, Buyan MI, Makievskaya CI, Buyan AI, Cherkesova KS et al. Sex-Specific effects of estradiol and progesterone in ischemic kidney injury. Int J Mol Sci. 2024;25(6).
93. Xiong C, Jia Y, Wu X, Zhao Y, Yuan S, Yan F, et al. Early postoperative acetaminophen administration and severe acute kidney injury after cardiac surgery. Am J Kidney Dis. 2023;81(6):675–e831.
94. Oliveira BM, de Almeida LF, Deluque AL, Souza CS, Maciel ALD, Francescato HDC et al. Calcitriol reduces the inflammation, endothelial damage and oxidative stress in AKI caused by cisplatin. Int J Mol Sci. 2022;23(24).
95. Wang Y, Zhang M, Bi R, Su Y, Quan F, Lin Y, et al. ACSL4 deficiency confers protection against ferroptosis-mediated acute kidney injury. Redox Biol. 2022;51:102262.
96. Patil CN, Wallace K, LaMarca BD, Moulana M, Lopez-Ruiz A, Soljancic A, et al. Low-dose testosterone protects against renal ischemia-reperfusion injury by increasing renal IL-10-to-TNF-α ratio and attenuating T-cell infiltration. Am J Physiol Ren Physiol. 2016;311(2):F395–403.
97. Hukerikar N, Hingorani AD, Asselbergs FW, Finan C, Schmidt AF. Prioritising genetic findings for drug target identification and validation. Atherosclerosis. 2024;390:117462.
98. Fu K, Si S, Jin X, Zhang Y, Duong V, Cai Q, et al. Exploring antidiabetic drug targets as potential disease-modifying agents in osteoarthritis. EBioMedicine. 2024;107:105285.
99. Wallace C. Eliciting priors and relaxing the single causal variant assumption in colocalisation analyses. PLoS Genet. 2020;16(4):e1008720.
100. Wu J, Chen X, Li R, Lu Q, Ba Y, Fang J et al. Identifying genetic determinants of sarcopenia-related traits: a Mendelian randomization study of druggable genes. Metabolism - Clin Experimental. 2024;160.
101. Hu M, Cebola I, Carrat G, Jiang S, Nawaz S, Khamis A, et al. Chromatin 3D interaction analysis of the STARD10 locus unveils FCHSD2 as a regulator of insulin secretion. Cell Rep. 2021;34(5):108703.

102. Fair BJ, Blake LE, Sarkar A, Pavlovic BJ, Cuevas C, Gilad Y. Gene expression variability in human and chimpanzee populations share common determinants. Elife. 2020;9.
103. Balasubramanian D, Borges Pinto P, Grasso A, Vincent S, Tarayre H, Lajoignie D, et al. Enhancer-promoter interactions can form independently of genomic distance and be functional across TAD boundaries. Nucleic Acids Res. 2024;52(4):1702–19.
104. Joshi PK, Pirastu N, Kentistou KA, Fischer K, Hofer E, Schraut KE, et al. Genome-wide meta-analysis associates HLA-DQA1/DRB1 and LPA and lifestyle factors with human longevity. Nat Commun. 2017;8(1):910.
105. Qiu X, Guo R, Wang Y, Zheng S, Wang B, Gong Y. Mendelian randomization reveals potential causal relationships between cellular senescence-related genes and multiple cancer risks. Commun Biol. 2024;7(1):1069.
106. Zhou S, Tao B, Guo Y, Gu J, Li H, Zou C, et al. Integrating plasma protein-centric multi-omics to identify potential therapeutic targets for pancreatic cancer. J Transl Med. 2024;22(1):557.
107. Nakao T, Bick AG, Taub MA, Zekavat SM, Uddin MM, Niroula A, et al. Mendelian randomization supports bidirectional causality between telomere length and clonal hematopoiesis of indeterminate potential. Sci Adv. 2022;8(14):eabl6579.

Publisher's note

Springer Nature remains neutral with regard to jurisdictional claims in published maps and institutional affiliations.